TKN **Telecommunication Networks Group**

Technical University Berlin

Telecommunication Networks Group

Virtual Optical Bus: A Novel Packet-Based Architecture for Optical Transport Networks

Ahmad Rostami

ahmad.rostami@tu-berlin.de

Berlin, February 2010

TKN Technical Report TKN-10-002

TKN Technical Reports Series

Editor: Prof. Dr.-Ing. Adam Wolisz

Abstract

We present virtual optical bus (VOB) as a novel architecture for packet-based optical trans-
port network. VOB is an evolutionary networking architecture based on optical burst/packet
switching (OBS/OPS) paradigm with a higher performance–in terms of packet loss rate and
network throughput. In the VOB architecture, aggregate traffic flows are grouped into clus-
ters and within each of the clusters a special form of coordination on packet transmission
is introduced. This leads to a great reduction of packet collisions in the network and also
an increase in the network throughput. Design issues related to the VOB architecture are
discussed and through two design examples the high potential of this approach in suppressing
the collisions inside the network is demonstrated.

Contents

Chapter 1

Introduction

The exponential growth of traffic in the Internet has turned optics into the technology of choice for transmission in the core of the network. In addition, it has created some concerns over the scalability of electronic switching, thereby pushing towards all-optical networks. Nonetheless, optics does not provide a good support for packet switching. Specifically, there are three major issues hindering realization of an all-optical packet switching approach in the near future: low speed of all-optical switches, immature all-optical processors and lack of true optical buffers. One promising approach to addressing these issues is optical burst switching (OBS), see [Qiao 99]–[Turn 99]. OBS consists in grouping packets into bursts, out-of-band signaling and cut-through switching that collectively eliminate the need for fast optical switches and all-optical processors. It however fails to fully eliminate the problem of buffering in the network. In fact, buffers are needed in packet switched networks for two purposes. First, they are used to keep the packets in nodes while the node controllers read and process the packets' headers. Additionally, buffers are the main tools to mitigate the contention problem over the output ports of packet switches. Although OBS eliminates the need to buffers with regards to their first role, it does not provide an efficient solution for contention resolution.

In our earlier work in [Rost 07], we demonstrated that in a transport network based on the OBS, traffic shaping at the entrance edge of the network offers high potential for contention mitigation. More specifically, the losses due to lack of buffers in transit switches are reduced by buffering–shaping–of data packets at the ingress edge of the network, where we can still use inexpensive electrical buffers. In this work we aim at even more efficient contention reduction by suggesting a novel architecture and protocol for optical transport network. In our approach, several ingress nodes inside the network are joined together to form an optical path that is termed *virtual optical bus* (VOB). A path formed in this way is called a virtual bus since the physical links to which a path is associated can be used by several paths simultaneously. A form of coordination among nodes belonging to the same VOB on injecting their packets into the network is applied to eliminate the potential of collisions among packets within the same VOB. In a VOB network–a network that applies the VOB approach–all flows are grouped into VOBs in such a way that each flow belongs to only one VOB and the flows belonging to different VOBs have the minimum potential for contention with each other inside the network.

The rest of this report is structured as follows. In the next chapter, we present architecture

TKN-10-002   Page 2

of the system under consideration and specify the VOB. In Chapter 3 we study the VOB network design problem and present an ILP formulation for that. Chapter 4 investigates the performance of VOB. Chapter 5 presents two examples of VOB network design to demonstrate effectiveness of VOB architecture in controlling the collisions. In Chapter 6 we present related work and finally, we conclude the report by outlining the future work in Chapter 7.

TKN-10-002   Page 3

Chapter 2

Virtual Optical Bus

2.1 System Architecture and Outline of Solution

Consider an OBS transport network having N nodes and L unidirectional WDM links, where links connect nodes following an arbitrary topology, e.g. [Qiao 99]. Any given link l can support W_l wavelength channels, each operating at rate C Gb/s.

The network operates in the asynchronous burst switching mode, where bursts (i.e. jumbo data packets destined to the same target node) are assembled at the edge node, and injected into the network. The information required by the intermediate nodes to forward a data packet towards its destination is carried in a separate header packet, which is released to the network simultaneously with the data packet but on a separate signaling channel, i.e., out-of-band signaling. At each intermediate node data bursts go through a tiny optical delay line while the header packet is converted to electrical domain, processed by the node controller and converted again back to optics (O/E/O conversion), see Fig. 2.1.

Each node n in the network is equipped with T_n tunable optical transmitters and R_n tunable optical receivers. Each tunable transmitter and receiver could be tuned to, respectively, send or receive data on any of the wavelength channels of the links attached to the node. Furthermore, a reactive contention resolution mechanism is implemented in each node n, which incorporates a set of G_n internal wavelength changers as well as F_n WDM fiber delay lines (FDL) per output link of that node. Note that, if a node operates only as a transit node, it does not need to contain any add/drop facilities. Similarly, if a node is only an edge node it does not need any wavelength changer or FDL buffer. Fig. 2.1 shows an abstract model of the node that can operate alternatively as an ingress/egress edge node and as a transit node.

Let us assume temporarily that the ingress nodes work independently–with no coordination among each other–for injecting traffic into the network, which is natural for packet switching paradigm. This carries a natural potential of collision among packets in the network. A collision occurs when two or more data packets are going to use the same channel on a given link for an overlapping period of time.

In the electronic packet-switched networks efficient avoidance of this adverse phenomenon is usually done by introducing some buffers that hold colliding packets during times of contentions. Unfortunately, the all-optical nodes have limited buffering potential–through FDL buffers–which due to lack of random access property can offer only pre-defined fixed delay

TKN-10-002 Page 4
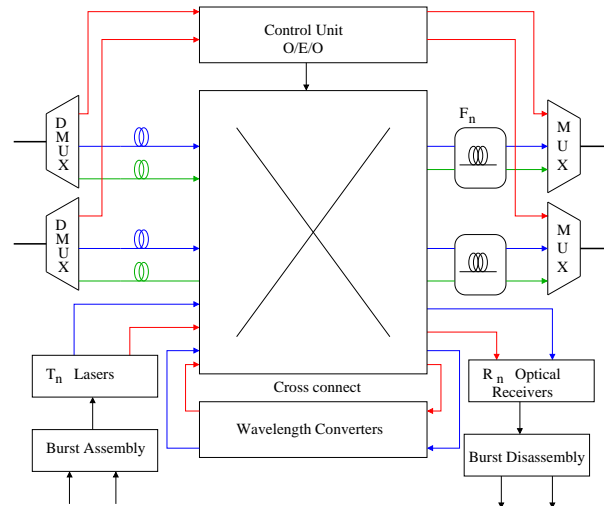
Figure 2.1: Abstract model of the switch assumed in our framework.

values. Accordingly, the only way to limit the contention is an appropriate traffic shaping at the input edge of the network. An optimal idealistic approach for this purpose would be global scheduling of all sources so that every single packet transmission from any source in the network is coordinated with all other sources so as to avoid collision in the transit nodes. This could–theoretically–be realized by introducing a central controller to the network that schedules all packet transmissions in the network in a collision-free manner. In this way, up to some maximum utilization the controller can assure that the packet will not collide with any other packet along its path to destination. Although this approach would potentially lead to the highest throughput in the network and the minimum amount of collisions, this might be too costly and not practical due to the necessary ideal time synchronization of all components, complexity as well as signaling and scheduling overhead. A natural alternative is going for decomposition of the global scheduling of all sources into smaller sets with local scheduling within each set and hoping that the results of the local scheduling will not collide too much with each other. Taking this into account, we postulate grouping of traffic sources into disjoint clusters and apply a form of coordination–traffic shaping–among associated sources in each cluster. In this way only the groups of sources remain independent and subject to collisions, thus reducing the collision rate in the network.

A crucial issue for clustering is setting the requirements for assigning sources to clusters. Taking into account that the final goal is to decrease the packet collisions in the network, a natural requirement is to form a cluster out of the sources that potentially share the same set of links in their path and thus their packets are likely to collide with each other. Furthermore, we have to take care that the sets of routes of flows from different clusters should intersect minimally–ideally be disjoint. In the latter case there would be–by definition–no collisions between the sources belonging to different clusters either! This might, however, be impossible in reality, thus we suggest keeping the inter-cluster collisions on a low level by finding for them paths with minimal interaction.

Concerning the scheduling within the clusters we target a distributed local scheduling mechanism rather than a centralized approach. As for the efficiency, the same criteria are applied to the local scheduling as the global scheduling. That is, a local scheduling algorithm operating on a local set of sources should schedule the corresponding packets with minimum–ideally no–collisions within that local set.

To evaluate the effectiveness of our approach in improving the performance of the network we consider three metrics: packet loss rate, access delay of packets and network throughput. Packet loss rate will be calculated as the fraction of generated packets by the ingress nodes that are lost in the network due to collisions. The access delay is calculated as the difference between the time a packet is generated by an ingress node and the time it is released to the network, and is calculated for successfully delivered packets. The maximum achievable throughput of the network will also be evaluated and compared with that of a conventional OBS network.

2.2 Virtual Optical Bus Description

Our approach for coordination of flows within each cluster will be based on the abstraction of the virtual optical bus (VOB)–a virtual unidirectional bus accommodating a set of O-D flows, defined as a flow of packets originated at an ingress edge node destined to a specific egress node in the considered network, on their entire route.

The following features collectively give the formal definition of the VOB.

- A VOB is defined over a specified sequence of connected links, i.e., it is a directed simple path.

- Each VOB is piecewise associated with a specific wavelength channel. On a multichannel link with wavelength changers available, a VOB can use any channel on that link; however, flows associated with that VOB may not use more than one channel at any given time.

- Each O-D flow must be associated with one and only one VOB.

Note that the third feature implies that both origin and destination of a given flow should be associated to the same VOB, i.e., traffic of an O-D flow will not be split/switched over multiple VOBs.

Following the description given above, establishing the coordination among flows associated to a VOB is now translated into designing a medium access control (MAC) protocol that ensures a collision-free, efficient and fair access to the VOB for the associated traffic flows. For this purpose we use a MAC protocol that is based on buffer-insertion protocol, which was first introduced in mid 80s and was afterwards improved and used in many other works, see [As 94]. In the buffer-insertion, each intermediate active node on a bus–an intermediate node that injects traffic into the bus–is equipped with an extra buffer called insertion buffer. The buffer is used to actively delay transit packets flowing on the bus in order to avoid them from colliding with local packets in transmission. Also, at every intermediate node priority is given to the transit traffic over the local traffic. In this way, the required capacity of the

TKN-10-002   Page 6
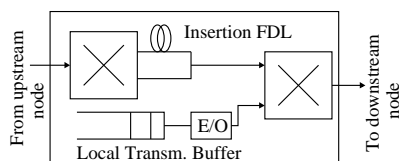
Figure 2.2: Abstract model of a single ingress node equipped with a FDL insertion buffer on transit path.

insertion buffer would be small. Specifically, it must hold a transit packet until the transmission of an ongoing local packet is completed; therefore, it only needs the capacity equal to the transmission time of a maximum-length packet.

In order to adopt the buffer-insertion protocol in the VOB, we need an insertion buffer per VOB per any active intermediate node being part of that VOB. That is, in a network with N nodes each node would require at most $N-1$ insertion buffer since it generates traffic destined to at most $N-1$ other nodes in the network. Since the insertion-buffer is used to buffer transit optical packets already traveling over the bus, it must be realized in the optical domain to avoid the need for the electro-optical conversion. Taking into account that the required capacity of an insertion buffer is small, it can be easily realized by single FDL as shown in Fig. 2.2.

A known phenomenon associated with the insertion-buffer protocol is the fairness issue. In fact, in a physical bus using insertion-buffer MAC protocol those nodes closer to the beginning point of the bus have better and faster access to the VOB. This might result in an unfair access to the bus for the nodes closer to the end of the bus. Nevertheless, this is not the case for the VOB MAC protocol. The reason lies in the fact that O-D flows are associated with a VOB based on their average data rate; that is, it is assumed that a single upstream node does not have the potential to monopolize the VOB in long term. Nevertheless, in order to guarantee that downstream O-D flows do not have to wait excessively long times before they are granted access to the VOB, in our design each source node in the network is further equipped with a token bucket shaper.

In a VOB using insertion-buffer MAC protocol transmission of packets is scheduled as follows. The most upstream ingress node of the VOB can inject traffic into the VOB any time that corresponding transmission channel is idle and there are enough tokens available. If a node is an active intermediate node it has to inject traffic into the VOB considering the status of the insertion buffer and the availability of tokens. Specifically, a local packet at the head of the local transmit queue is transmitted over the channel as soon as both the channel and the insertion buffer are idle and there are enough tokens available. If a transit packet arrives during transmission of a local packet, it is simply delayed by the insertion FDL. When a transit packet is put in the FDL, all upcoming transit packets go through the insertion FDL until a transit packet arrives and finds the channel in the idle state. In that case, the packet bypasses the insertion-buffer and immediately receives service. This operation guarantees a collision-free packet transmission within a VOB.

To elaborate more about the VOB operation let us now make an example. Fig. 2.3 depicts a network with 5 nodes, in which nodes 1–4 generate traffic destined to node 5 each with the

TKN-10-002   Page 7
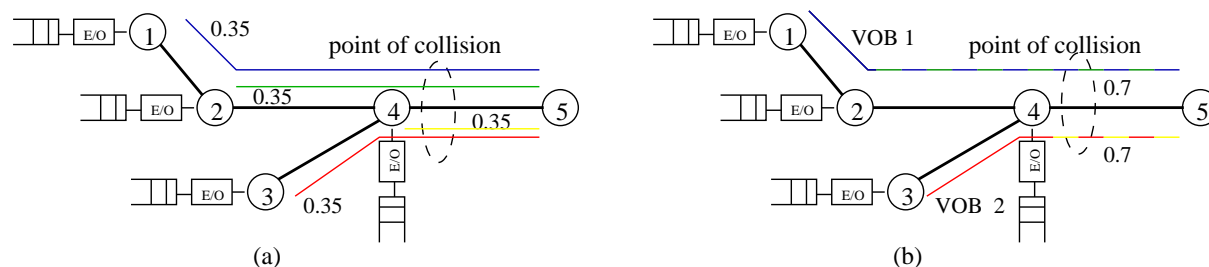
Figure 2.3: An example of applying the VOB Framework, (a) a simple network with 4 O-D flows, (b) the same network after applying the VOB framework.

intensity equal to 0.35 of the capacity of a single WDM channel. Packets generated at each node go through an electro-optical (E/O) conversion before transmission. The link $(4 \to 5)$ is offered the load of 1.4 through multiplexing four independent O-D flows. If we suppose that this link has two data channels and two tunable wavelength changers with no FDL buffer and that traffic of each source is injected according to the Poisson process, by applying the known Erlang-B formulae [Akim 99] we observe some 29% packet loss rate over this link under OBS operation. Now, we establish two VOBs over the physical routes $(1 \to 2 \to 4 \to 5)$ and $(3 \to 4 \to 5)$, respectively (Fig. 2.3-b). The former VOB accommodates O-D flows $(1 \to 5$ and $2 \to 5)$ and the latter one carries the traffic of O-D flows $(3 \to 5$ and $4 \to 5)$. In this case, by using the MAC protocol described above node 2 (4) will schedule its local packets in a way that they do not overlap with packets of node 1 (3), i.e., no intra-VOB collision occurs. Consequently, we only have two independent traffic flows being multiplexed into the link $(4 \to 5)$ and therefore no packet collision will occur on this link anymore since it already has two channels.

Chapter 3

VOB Network Design

Design of a VOB network consists of grouping all O-D flows into VOBs and that has to be done with the objective of minimizing packet collision rate in the network. We refer to this step as VOB layout design, which can formally be stated as follow. Having a network with given resources, as explained in Chapter 2, and an O-D traffic matrix, how to cover the traffic matrix by a set of VOBs, with respect to the limitations imposed by the topology and the resources available within each node and link, in such a way that the packet collision in the network is minimized. The VOB layout design should give us complete information about the beginning, the end and the route of all VOBs as well as the ids of flows to be covered by each VOB. It should be noted that VOB layout design involves assigning O-D flows to VOBs and that, in turn, implies routing of O-D flows in the network.

Taking into account that the intra-cluster collisions–collisions among the flows belonging to the same VOB–are completely suppressed by the proposed MAC protocol, the objective function of the VOB layout design translates into minimizing the inter-cluster collisions across the network. Nevertheless, minimization of the inter-cluster collisions cannot be explicitly formulated in a straightforward manner, if at all possible, since it depends on many factors such as traffic characteristics and routing. Consequently, we resort to implicit formulation of the objective function and set it to minimization of maximum number of VOBs that are multiplexed to any link in the VOB network. This objective function will minimize the interaction among routes of VOBs in the network, thereby reduces the inter-cluster collision across the network. In the following, we apply the path-based method [Pior 04] to formulate the VOB layout design as an integer linear programming (ILP) problem.

3.1 Preprocessing

The optimization includes a preprocessing phase that facilitates the VOB layout design. The preprocessing is responsible for generating a list of many potential VOBs in the network, and for each potential VOB determining all O-D flows that it could support.

Let us assume that all links and O-D flows in the network are, respectively, populated in set $\mathbb{L}$ with L elements, and $\mathbb{F}$ with F elements. We first apply the k-shortest path (KSP) routing algorithm [Epps 99] to the given topology and populate the set of all k-shortest paths between all pairs of nodes in the network in $\mathbb{P}$ with size P. Note that $\mathbb{P}$ is the set of VOB

candidates in the network.

Now we form the matrix Θ $(P \times L)$ that relates links in the network to the paths populated in $\mathbb{P}$. That is,

$$\theta(p, l) := \begin{cases} 1 & \text{if link } l \in \mathbb{P} \text{ is used in path } p \in \mathbb{P}, \\ 0 & \text{otherwise.} \end{cases}$$

In the next step, we form Γ, which is an $P \times L \times F$ matrix, and whose elements are calculated as:

$$\gamma(p, l, f) := \begin{cases} 1 & \text{if O-D flow } f \in \mathbb{F} \text{ could be supported} \\ & \text{by path } p \in \mathbb{P} \text{ on link } l \in \mathbb{L}, \\ 0 & \text{otherwise.} \end{cases}$$

In case there are any constraints regarding the routing of some O-D flows in the network they have to applied during the formation of Γ. One such constraints can be the maximum allowable hop count for routing of O-D flows. We finally note that for a given network topology the preprocessing phase needs to be done only once.

3.2 ILP Formulation

3.2.1 Assumptions

For our formulation we make the assumption that all nodes support full wavelength conversion. Note that, this is not mandatory for the VOB design framework, and we only make the assumption here since it will improve the performance and further simplify the design of the layout.

3.2.2 Parameters and Variables

The parameters used in the formulation are the followings:

- $\Lambda = [\lambda^f]$ is the given demand matrix, where λ^f denotes the intensity of the O-D flow $f \in \mathbb{F}$ (normalized to the wavelength capacity).

- $\rho_{max,w}$ is the maximum allowable load on a single WDM channel in the network.

Also, the variables are:

- x_p

$$x_p := \begin{cases} 1 & \text{if path p} \in \mathbb{P} \text{ is a VOB}, \\ 0 & \text{otherwise.} \end{cases}$$

- y_p^f

$$y_p^f := \begin{cases} 1 & \text{if flow f} \in \mathbb{F} \text{ is supported by path p} \in \mathbb{P} , \\ 0 & \text{otherwise.} \end{cases}$$

3.2.3 Objective Function

We set the ILP objective function to

$$Min \ \max_{l \in \mathbb{L}} \sum_{p \in \mathbb{P}} \theta(p,l) x_p. \tag{3.1}$$

The objective function minimizes the maximum number of multiplexing VOBs over any link in the network.

3.2.4 Optimization Constraints

$$\sum_{p \in \mathbb{P}} y_p^f = 1 \qquad \forall f \in \mathbb{F} \tag{3.2}$$

$$\sum_{f \in \mathbb{F}} y_p^f \lambda^f \gamma(p,l,f) \leq x_p \rho_{max,w} \qquad \forall l \in \mathbb{L}, p \in \mathbb{P} \tag{3.3}$$

In constraint 3.2 each traffic flow is associated to one and only one VOB. Also, constraint 3.3 assures that traffic offered to any part of a VOB on any link in the network does not exceed a fraction of WDM channel capacity equal to $\rho_{max,w}$, which is a design parameter used to control the access delay of traffic sources.

Chapter 4

Performance Analysis of VOB

In this chapter, we investigate the operation and performance of the VOB and compare it to those of conventional OBS. The VOB MAC protocol presented in Chapter 2 is a new variation of the well-studied buffer-insertion protocol. In the buffer-insertion, where a physical bus is shared among a set of nodes, 100 % throughput can be achieved as long as the total load offered to each segment of the shared bus is smaller than transmission capacity of that segment. The only concern would be delay of accessing the bus, which rapidly increases with the distance of a node from the head-end of the shared bus. This is the so-called fairness issue associated with the buffer-insertion protocol. The issue stems basically from the inherent priority of upstream sources in accessing the bus that allow them to grab as much capacity as they want without considering the needs of downstream nodes. Although, this can effectively be controlled by limiting the injection rate of each source to the bus, e.g., by means of a token bucket controller, one cannot achieve 100 % throughput under load-controlled insertion-buffer protocol owing to the fact that FDL-based insertion-buffer cannot utilize the whole capacity of an optical link. That the type buffer used in realizing the FDL-based insertion buffer does not support random access property leads to the fragmentation of data channel and this consequently hinders the optimum utilization of channel capacity. Therefore, it is of great importance to investigate the delay-throughput characteristics of the MAC protocol proposed for the VOB.

To investigate the operation of VOB we consider a general scenario as depicted in Fig. 4.1. The network under consideration consists of B parallel branches, $(n+1) \times B + 1$ nodes and $(n+1) \times B$ unidirectional links, where a link connecting node l to node m is realized by a WDM link with $W_{l,m}$ data channels and one control channel. The network in Fig. 4.1 is designed in a way that we can characterize the performance of VOB under a wide range of combinations of traffic intensity, number of nodes, number of wavelength channels and network topologies. Accordingly, in our study we vary the load offered by each source node, B and n. For our evaluations, we further make the following assumptions:

- The nodes located on the left side of link L generate traffic destined to a node in the right side of link L. More precisely, nodes $S_{i,1}, ..., S_{i,n+1}$ generate traffic for node D_i $(i \le B)$.

- Sum of generated load by all nodes destined to node D_b $(1 \le b \le B)$ is less than the transmission capacity of a single wavelength channel.
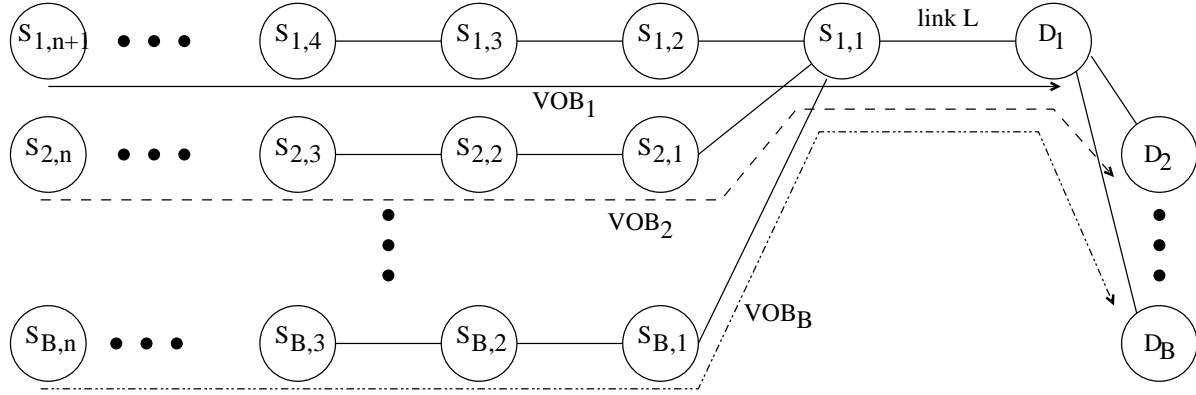
Figure 4.1: Network Topology for MAC Protocol Evaluation.

- The network operates under either of the two modes: OBS and VOB. In the latter case, one VOB is established on any branch b ($b \leq B$) and all sources over the branch are associated to that VOB, see Fig. 4.1 . Accordingly in this case each active node on the VOB is equipped with the VOB MAC protocol and corresponding FDL-based insertion buffer.

- Number of wavelength channels on links at the left side of the link L, on link L and on links at the right side of the link L are equal to n, W_L and 1, respectively.

- Each source node is equipped with one tunable optical transmitter, n tunable wavelength converter and it does not have any FDL buffer.

- At each source node bursts of fixed length are generated according to the Poisson process with intensity ρ, as normalized to wavelength channel capacity.

4.1 Simulation Experiments and Discussion

We evaluate the scenario explained above through discrete-event simulation experiments conducted in OMNeT++ [Varg 06]. In our experiments we set wavelength channel capacity and burst length to 10 Gb/s and 10 kB, respectively. Also, for each simulation experiment 90 % confidence intervals for the corresponding measure is estimated, though to improve the readability of results they are omitted where they are too small.

Results of our experiments are depicted in Fig. 4.2-4.12, which show throughput, access delay and loss rate curves as function of load offered to link L for different combinations of B, n and W. In the following we discuss the achieved results in detail.

4.1.1 Loss Rate and Throughput

First let us consider loss rate and throughput of the network and evaluate impacts of load, n and B. First and foremost, we observe that the VOB greatly reduces the loss rates. In particular, a loss-free transport of data can be achieved under VOB as long as number of

Table 4.1: Throughput gain of VOB over OBS at 70% link load in per cent

	B=2		B=3		B=4		
	$W_L = 2$	$W_L = 1$	$W_L = 3$	$W_L = 2$	$W_L = 4$	$W_L = 3$	$W_L = 2$
n=2	16.5	2.9	13.0	7.4	7.0	8.0	4.1
n=3	19.7	5.3	15.6	9.1	9.2	9.4	5.4
n=4	22.2	5.7	16.7	10.0	10.1	10.0	6.1
n=6	22.7	8.8	17.8	10.4	10.9	10.6	6.9

VOBs associated with any link in the network is equal or smaller than number of wavelength channels supported by that link. This can lead to a higher throughput with VOB than with OBS. In fact, when there is no loss rate in the network, the throughput of 100% can be achieved. Table 4.1 summarizes the throughput gain of the considered network for the case that the link L is 70% loaded. It is seen that the the throughput gain of VOB can be as high as 22.71%.

Below we analyze impacts of different factors separately. In our discussion we distinguish between two modes of operation: mode I corresponding to the case where number of VOBs associated with link L is smaller than or equal to W_L and mode II referring to the other cases.

Offered Load

In mode of operation I the loss rate is always zero and independent of the load. In this mode, we observe the largest difference between the VOB and OBS in terms of the loss rate and the throughput. In mode II burst losses occur both in VOB and OBS, which also increase with the offered load. Nevertheless, the loss rate of VOB is much smaller than that of OBS. In addition, in this mode the difference between the two approaches in terms of the throughput increases with load.

Number of Nodes n

Again let us begin with the operation mode I. In this mode, the loss rate is zero that leads to 100% throughput and both throughput and loss rates are independent from the number of nodes n. However, this is node the case for OBS, in which both the loss rate and the throughput deteriorate with n. In other words, increasing n improves the gain in throughput and loss rate of VOB over OBS. In addition, it is seen that the deterioration of the OBS throughput with n is not linear. For instance, the reduction in throughput due to increasing n from 2 to 3 is much less than that due to increasing n from 3 to 4.

In mode II, similar to OBS, the throughput of VOB decreases with n for a given setting. Nevertheless, the reduction of throughput for VOB is much lesser than that of OBS. This again help the VOB to outperform OBS more largely with n.

More specifically, as the ratio number of VOBs on link n approaches to W_L, the deteriorating impact of n on VOB decreases (e.g., compare the cases B=4/W_L=3 and B=4/W_L=2) and as a result, the distinction between the throughput of VOB and OBS increases.

Number of VOBs

As long as number of wavelength channels W_L is larger than B, i.e., mode of operation is I, both loss rate and throughput are independent from B and are equal to zero and 100%, respectively. To compare the results of VOB with those of OBS we note that when B increases, W_L has to be increased too. Therefore, as seen in the figures at the same offered load on link L, the loss rate reduces with B, though the reduction is not noticeable. As a result, the difference between the throughputs of VOB and OBS at 70% link load reduces with B as depicted in Table 4.1.

In mode II the throughput gain achieved through using VOB depends very much on the ratio B/W_L as depicted in the figures. For instance, the throughput gains are very similar for cases $B = 4/W_L = 2$ and $B = 2/W_L = 1$. Additionally, the throughput gain of VOB improves as B/W_L approaches 1.

4.1.2 Access Delay

In the last section we studied the gain of VOB over OBS–in terms of throughput and loss rate. The gains come at the cost of increase in the time it take for a source node to inject its traffic into the network, i.e., the access delay. In this section, we evaluate the access delay in detail. Depicted in Figs. 4.10-4.12 are the access delay results for different combinations of n and B in mode I of operation. The access delays for VOB in mode II as well as for OBS network are all less than 10 μs and therefore not shown in figures. Depicted in each graph is the average delay values experienced by node $S_{1,1}$ before accessing VOB 1 against load and at at different positions of this node with respect to the head node in VOB 1. For example, node position 4 means that $n = 3$, i.e., the head node in VOB 1 is node $S_{1,4}$, thus the node $S_{1,1}$ has 3 upstream nodes associated with VOB 1.

First and foremost it is seen that the access delay for node $S_{1,1}$ at position 7 is still smaller than 150 μs for all values of B at the VOB load of 70-75%. It should be noted that the access delay in the range of 100-200 μs can be considered as acceptable taking into account the propagation delay in a metro/core network that is usually in the range of ms. More specifically, the access delays increase smoothly with VOB load up to a knee point, which occurs at offered load of around 60-65% for all the considered scenarios. For the load values beyond this point the access delays increase sharply. This is not the case for OBS where the loss rate is the dominant phenomenon when the load increases and a node can inject its packets to the network as soon as it finds a gap in the schedule of the channel without needing to coordinate its transmission with any other upstream node. Although the node position has a large impact on the access delay after the knee point, this impact is not large when the load offered to VOB is smaller than the load value at which the knee point occurs. Also, it is also not surprising to see that number of VOBs B does not affect the access delay to a large extent, since different VOBs are to a high extent isolated from each other as long as $\frac{W_L}{B} \geq 1$.

In mode II of operation the access delay is less than 10 μs under operation mode II even at 70-75% VOB load and node position 7. The reason is that for a given number of VOBs B to keep the load on the link fixed while decreasing W_L the load per VOB has to be reduced proportionally. The reduction in the VOB load, in turn, pushes the access delay curve under the knee point, where the access delay is small.
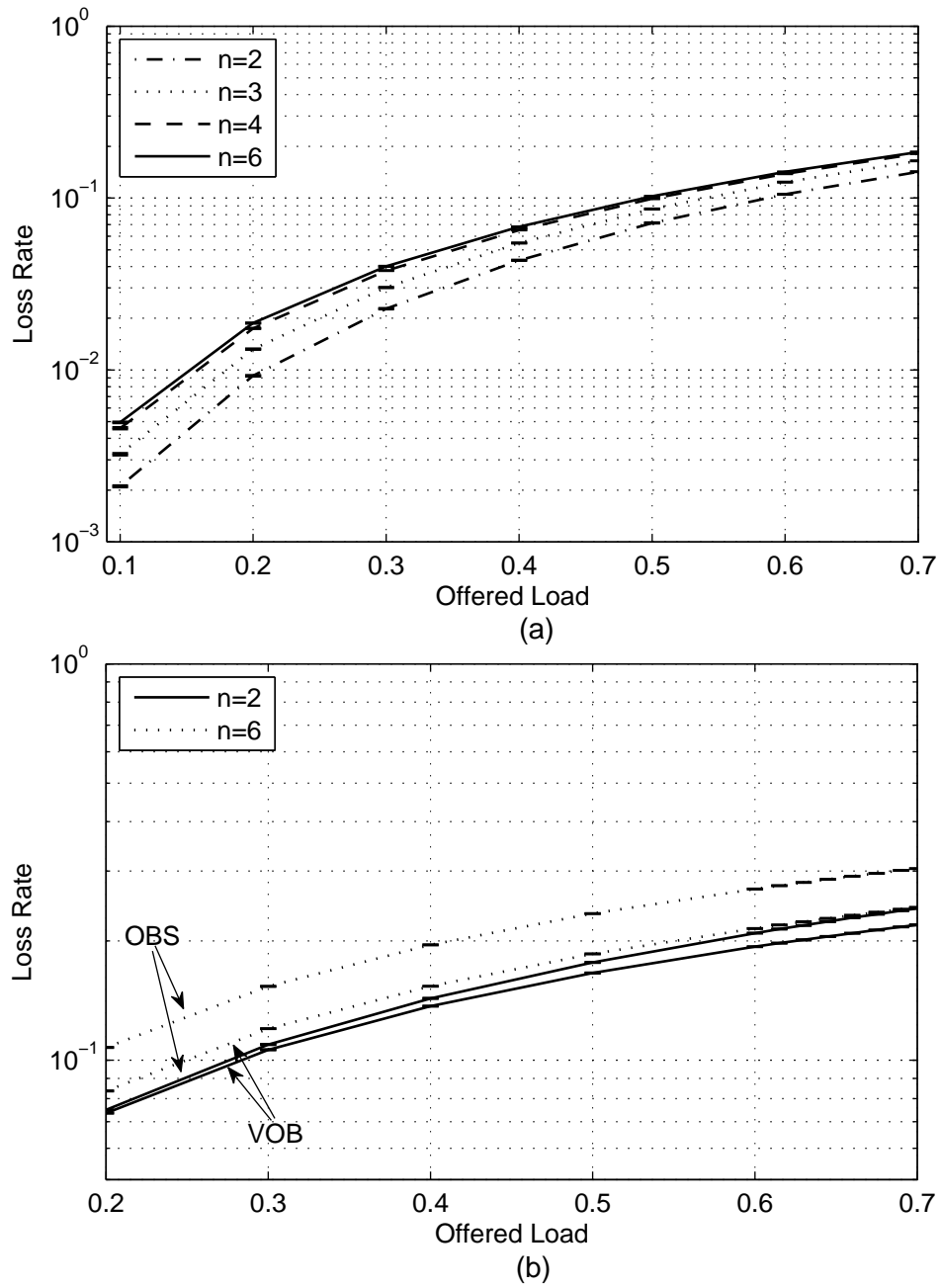
Figure 4.2: Loss rate over the link L against the offered load for B=2, (a) OBS, W=2. The loss rate for VOB is zero, (b) W=1.
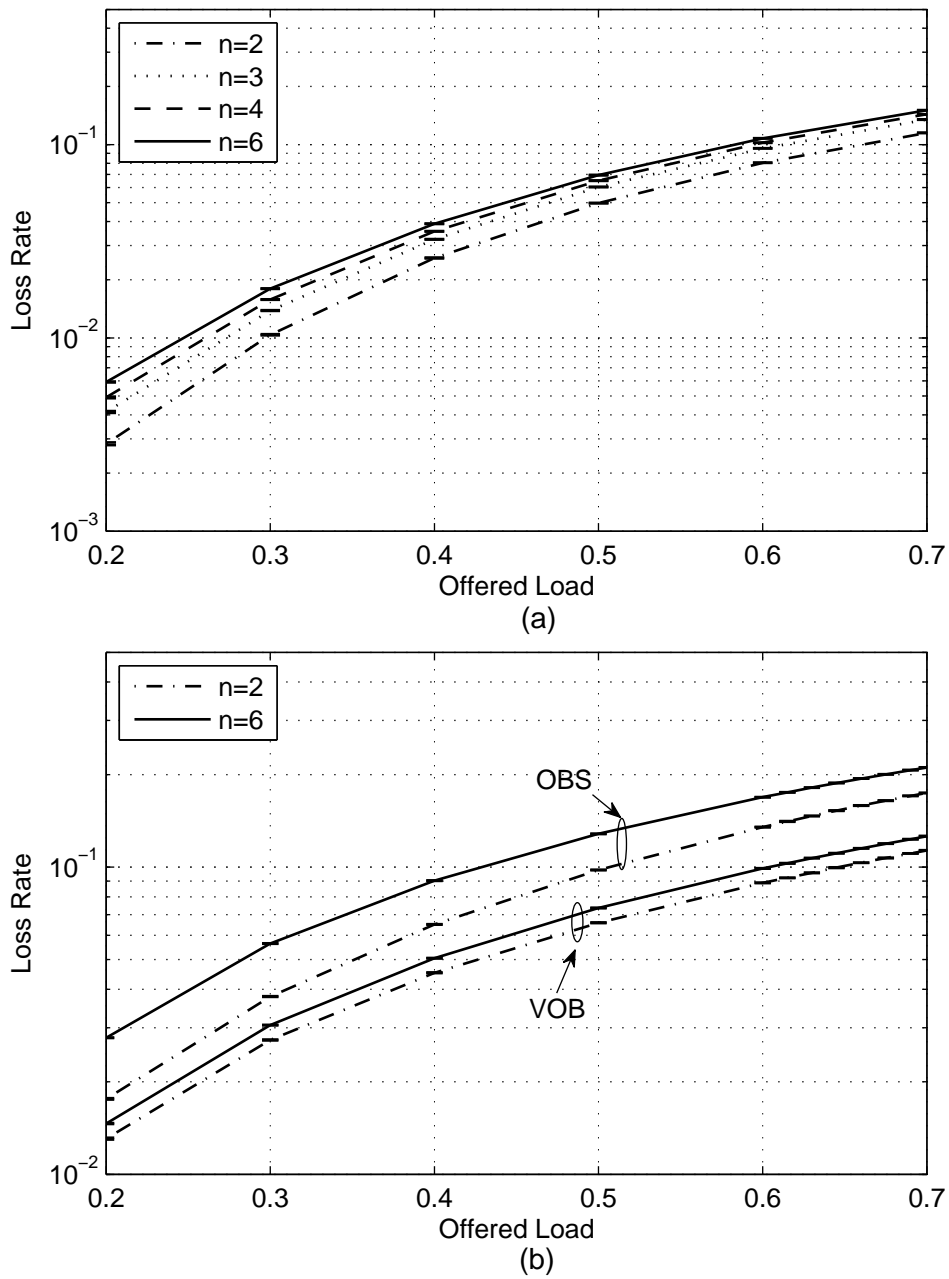
Figure 4.3: Loss rate over the link L against the offered load for B=3, (a) OBS, W=3. The loss rate for VOB is zero, (b) W=2.
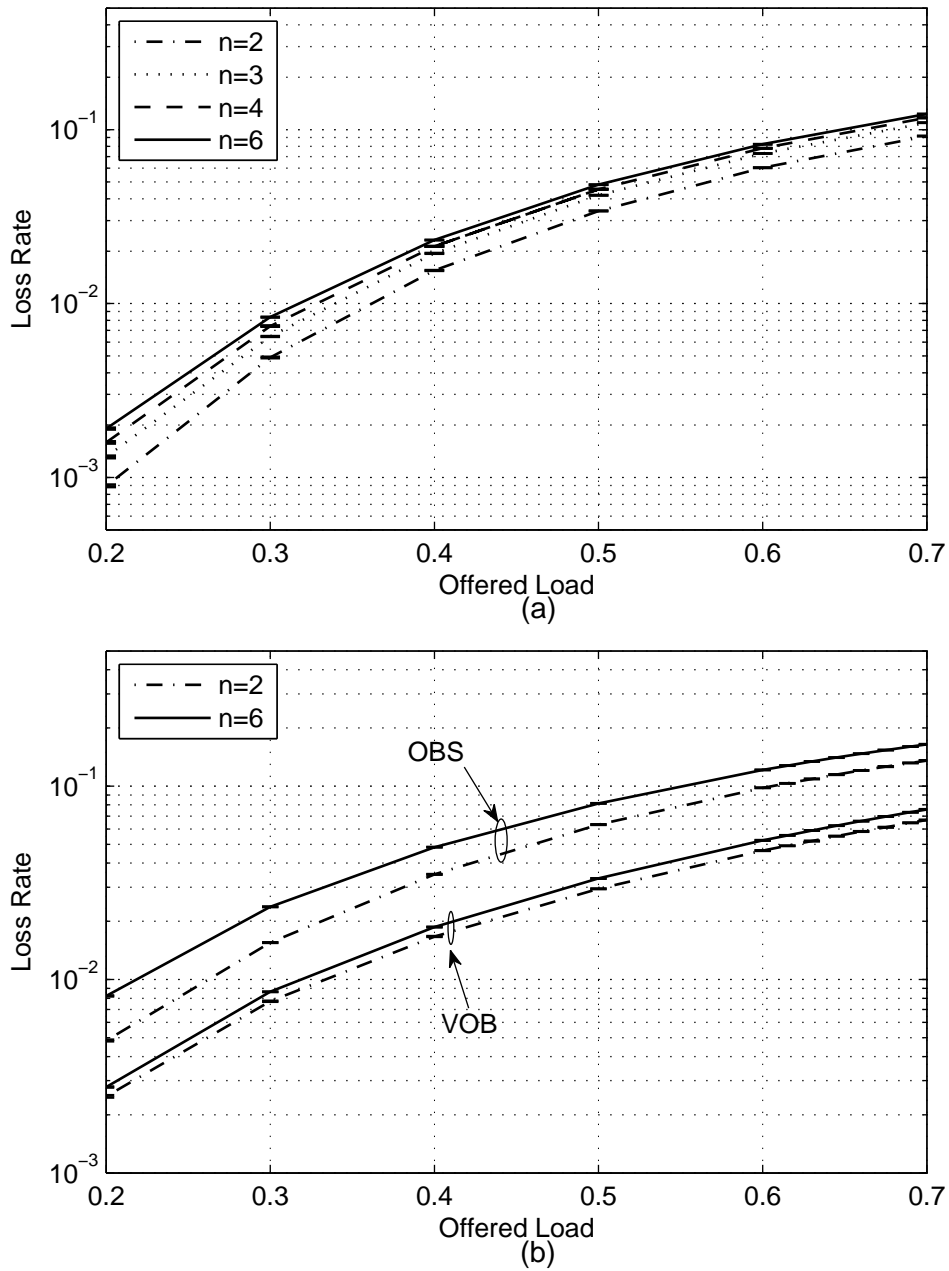
Figure 4.4: Loss rate over the link L against the offered load for B=4, (a) OBS, W=4. The loss rate for VOB is zero, (b) W=3.
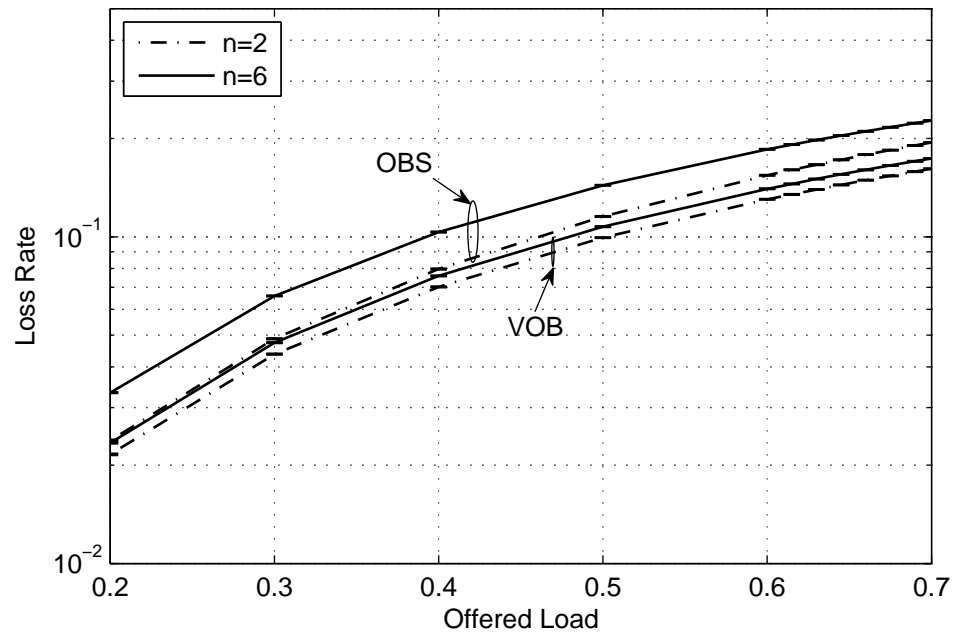
Figure 4.5: Loss rate over the link L against the offered load for B=4 and W=2.
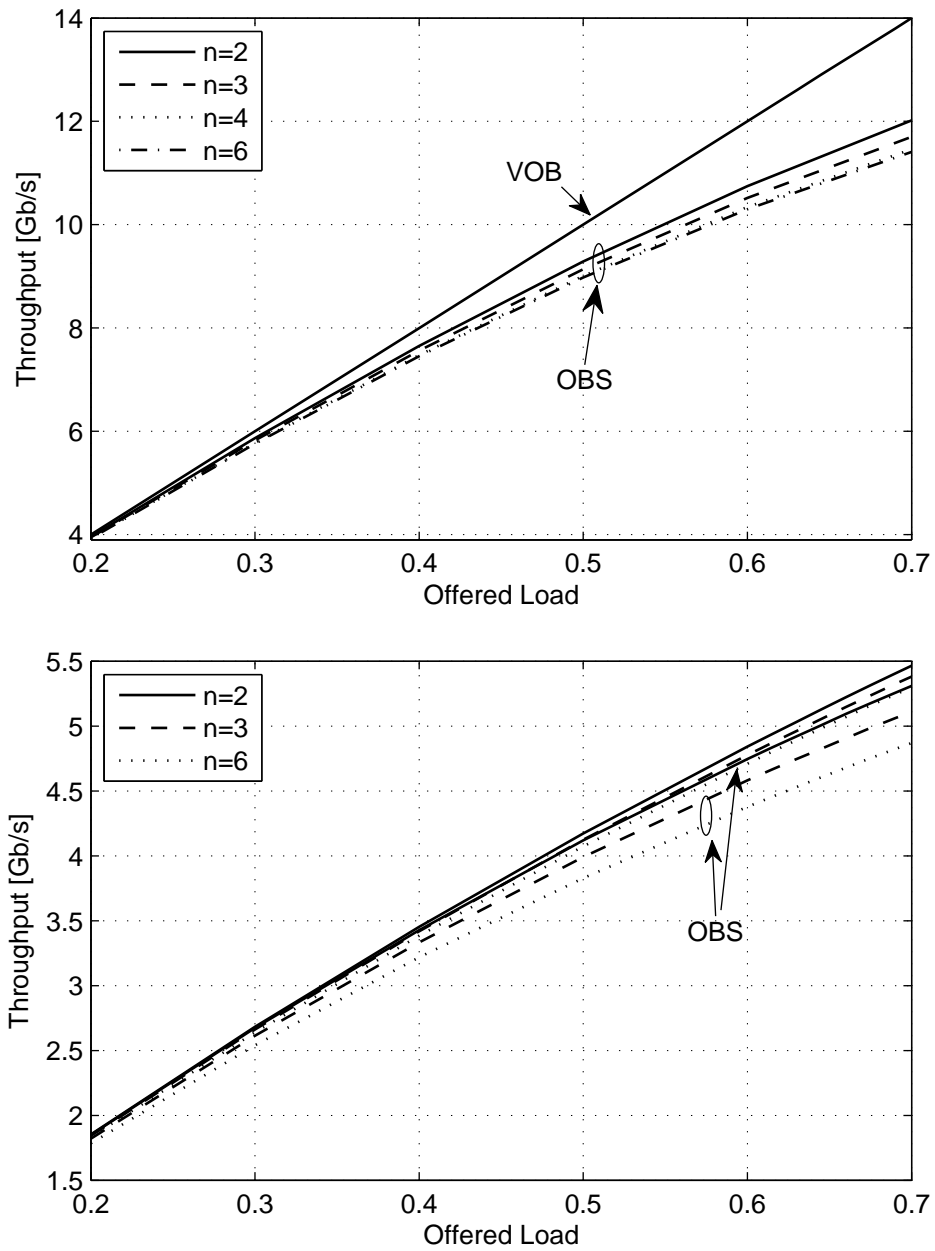
Figure 4.6: Throughput of the network against the offered load to link L for B= 2, (a)W=2, (b) W=1.
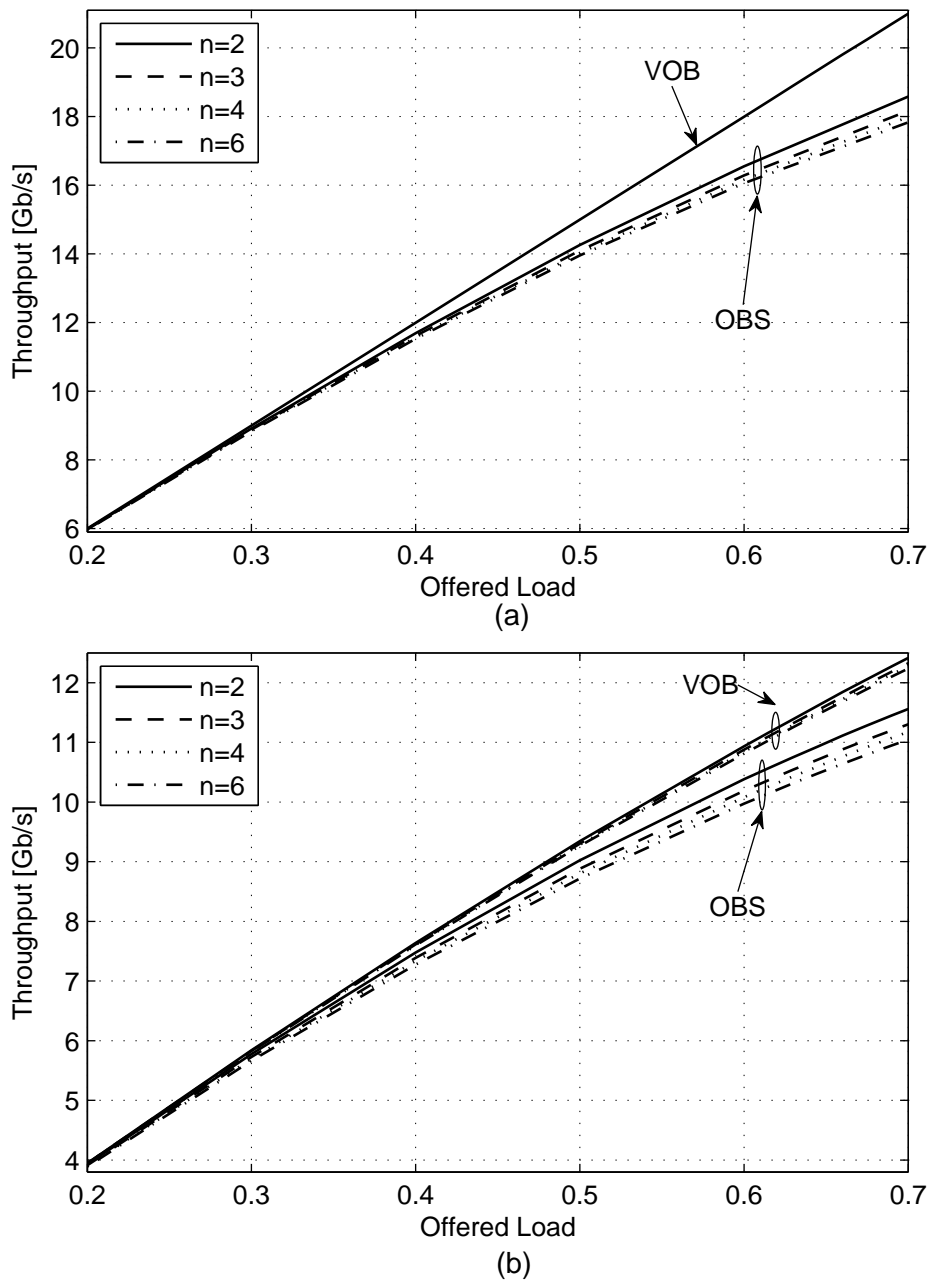
Figure 4.7: Throughput of the network against the offered load to link L for B= 3, (a)W=3, (b) W=2.
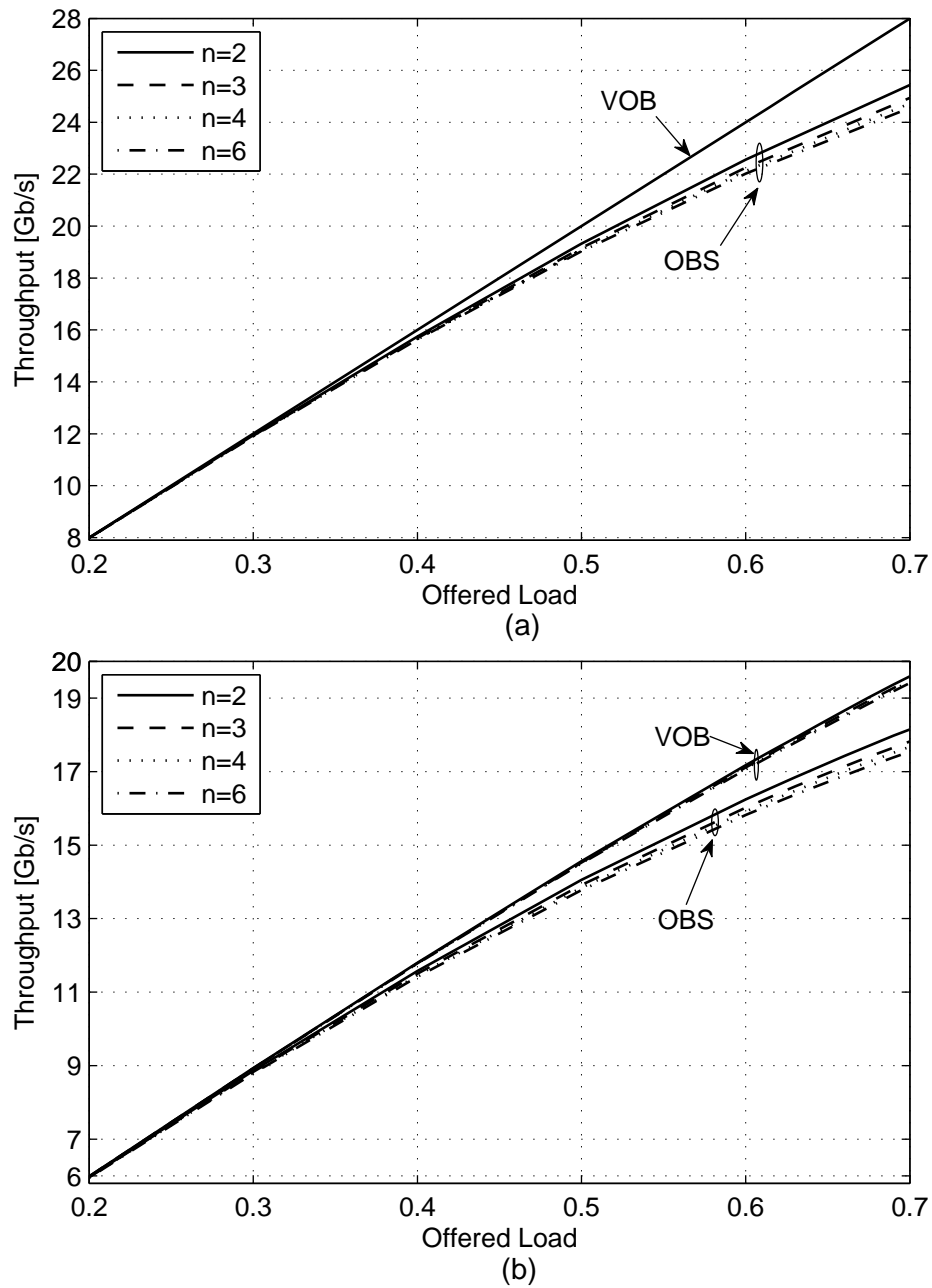
Figure 4.8: Throughput of the network against the offered load to link L for B= 4, (a)W=4, (b) W=3.
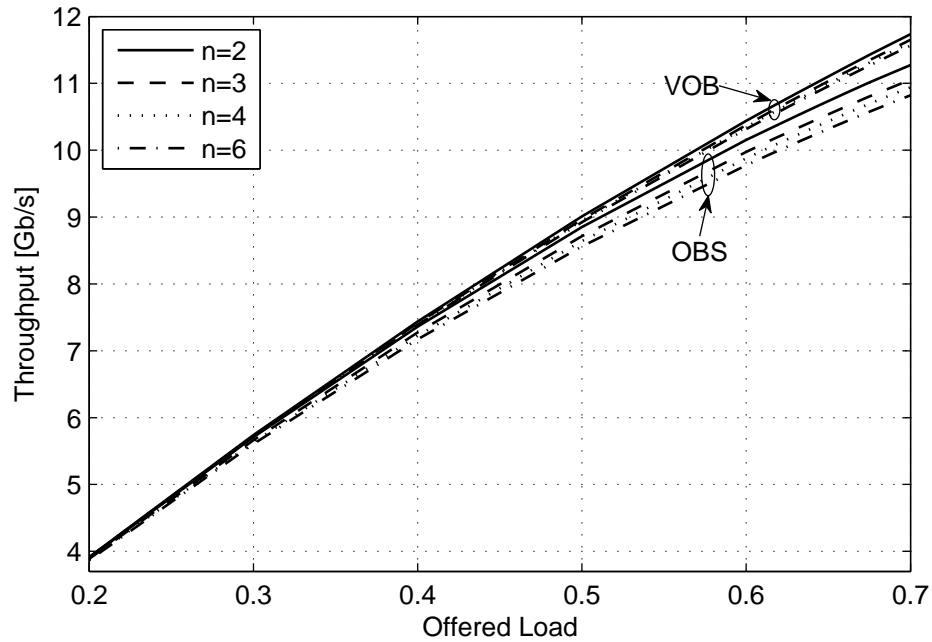
Figure 4.9: Throughput of the network against the offered load to link L for B= 4 and W=2.
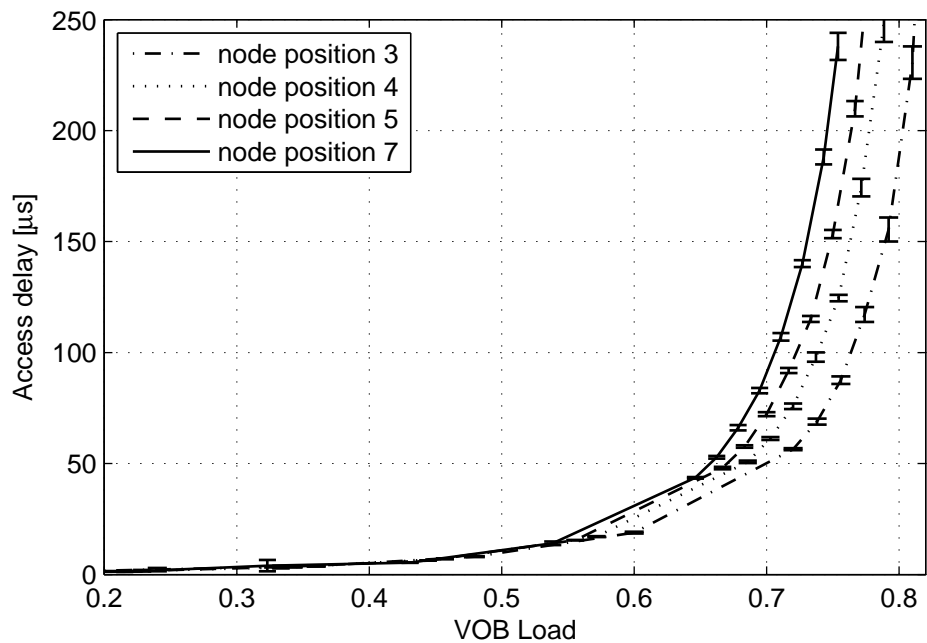
Figure 4.10: Access delay experienced by node $S_{1,1}$ in accessing VOB 1 at B=2 and W=2. Node position refers to the distance of node $S_{1,1}$ from the most upstream node in VOB.
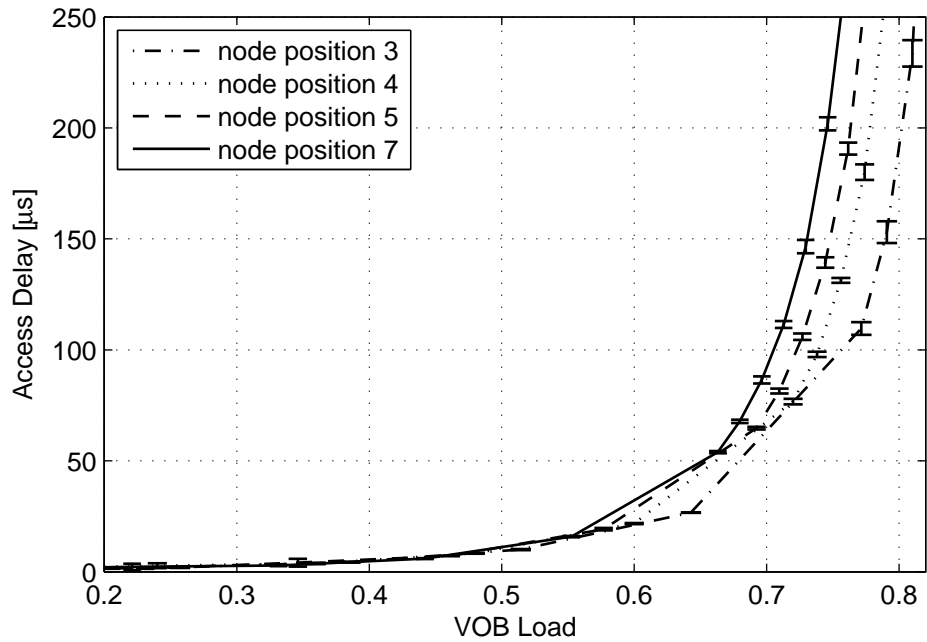
Figure 4.11: Access delay experienced by node $S_{1,1}$ in accessing VOB 1 at B=3 and W=3. Node position refers to the distance of node $S_{1,1}$ from the most upstream node in VOB.
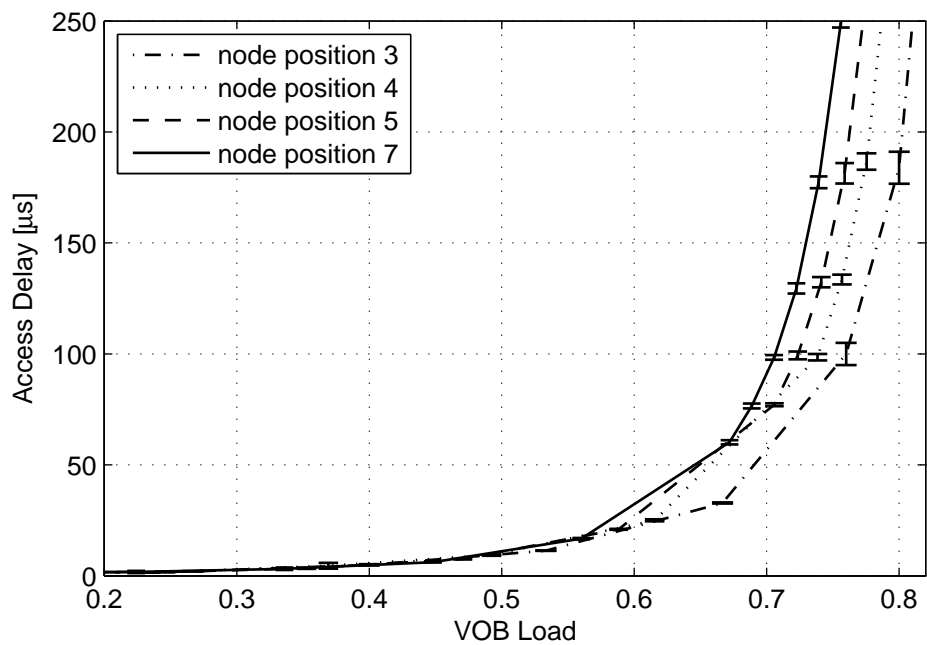
Figure 4.12: Access delay experienced by node $S_{1,1}$ in accessing VOB 1 at B=4 and W=4. Node position refers to the distance of node $S_{1,1}$ from the most upstream node in VOB.

Chapter 5

VOB Network Design Examples

In this chapter we present design examples of the VOB network and evaluate performance of designed networks. For this purpose, we consider two network topologies as explained below.

In the first design example, we consider a network with 10 nodes, where nodes are connected according to a bidirectional ring topology. Each node is connected to any of the two adjacent nodes via two WDM fibers in different directions, i.e., there are 20 fiber links in the network.

In the second example, the NSFNET backbone network with 14 nodes are considered, as depicted in Fig. 5.1. The network has 42 unidirectional fiber links and the minimum and maximum nodal degree of the nodes are 2 and 4, respectively.

In both networks it is assumed that each WDM link supports one control channel and four data channels, where each data channel operates at rate 10 Gb/s. The architecture of the nodes is the same as the one described Chapter 2. In the ring network, each node is equipped with $T_n = R_n = 8$ tunable lasers and receivers as well as $G_n = 8$ internal wavelength converters. As for the NSFNET, the number of available tunable lasers and receivers as well as that of wavelength converters in node i ($0 \le i \le 13$) is set to $T_n = R_n = 4 \times ND_i$ and $G_n = 4 \times ND_i$, respectively, where ND_i is the nodal degree of node i.
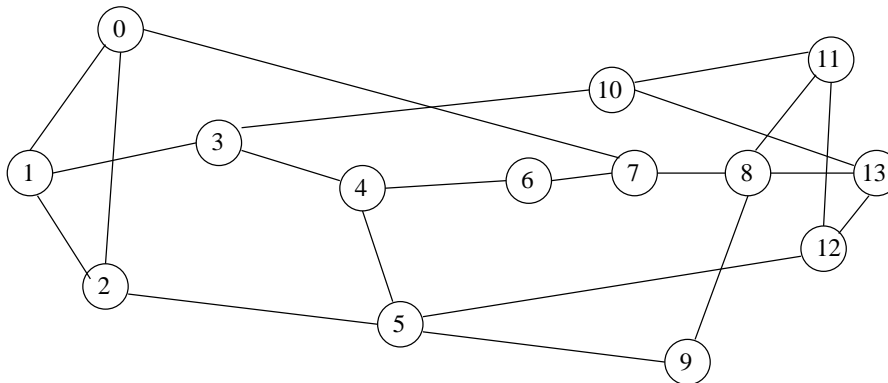
Figure 5.1: NSFNET Topology.

5.1 Solving the ILP

5.1.1 Ring Network

For the ring network illustrated above we generate two different traffic matrices. The first one is a random traffic matrix as depicted in Table 5.1. Each element in the matrix of Table 5.1 represents the average traffic demand between two corresponding nodes (O-D flow) as normalized to the capacity of a single wavelength. The traffic matrix has been generated in a way that all its elements are smaller than 0.4 and the average demand per O-D flow is 0.187. The second traffic matrix is a uniform one, where the demands of all O-D flows are the same and equal to 0.187. That is, the average demand per O-D flow is the same for both the traffic matrices. In the pre-processing phase both possible paths[1] for each source-destination pair are included $\mathbb{P}$. The commercial solver CPLEX 9.0 [Cple 03] is used to solve the ILP problem formulated in Section IV. Our analysis of the VOB in Chapter 4 suggested that the parameter ρ_{max_w} should be set to a value around 0.7 in order that all the traffic sources associated to a VOB experience a reasonable access delay. Accordingly, the ILP problem is solved for each of the two traffic matrices and with two values of the parameter ρ_{max_w}; 0.7 and 0.75.

A summary of the relevant characteristics of resulting VOB networks and a comparison with the corresponding OBS networks are depicted in Table 5.2. Details of the solutions are given in Table A.1-A.4 in Appendix A.

Depending on the used traffic matrix and the applied parameter ρ_{max_w}, the total number of VOBs required to support the demand matrix varies between 13 to 23, which indicates around 74.4% to 85.5% reduction in the number of independent flows in the network as compared to the OBS with 90 flows. Also, the average number of VOBs associated to a link in the network varies between 3.95 and 4.95, whereas in the OBS architecture 12.5 independent flows are associated to each link, in average. The VOB does not affect the average traffic load assigned to each link in the network noticeably, which implies that the routing of the traffic in the VOB network is not effectively different from the shortest path routing applied in OBS.

Now let us consider the difference between the solutions at the two values of ρ_{max_w}. In general, we expect that the number of VOBs per link in the network decreases with ρ_{max_w}. However, for the random traffic matrix, the average number of VOBs per link does not change when ρ_{max_w} is increased to 0.75. In fact, the impact of ρ_{max_w} on the average number of VOBs per link should be a step-wise relation, that is, there is a range of values of ρ_{max_w} over which the average number of VOBs per link remains unchanged. On the other hand, although setting the ρ_{max_w} to any value within this range does not affect the number of VOBs per link, we expect that it impacts the performance of the network. For example, in the considered scenarios the maximum number of VOBs per link in the network is 4 at both values of ρ_{max_w} for the random traffic matrix and as each link in the network supports 4 wavelength channels, the loss rate would be zero in the network at both values of ρ_{max_w}. However, we expect the access delay to be higher for $\rho_{max_w} = 0.75$ as the VOBs are more packed in this case as compared to the case with $\rho_{max_w} = 0.7$. As a conclusion, it would be better–in terms of the access delay–to design the VOB layout of a network at the minimum

---

[1]There are two candidate paths for each source-destination pair on a bidirectional ring topology.

Table 5.1: Random Traffic Matrix for the Ring Network used in the Design Example.

	1	2	3	4	5	6	7	8	9	10
1	0.000	0.180	0.043	0.173	0.341	0.167	0.312	0.094	0.219	0.372
2	0.318	0.000	0.385	0.364	0.249	0.020	0.156	0.141	0.119	0.310
3	0.124	0.092	0.000	0.073	0.140	0.361	0.097	0.328	0.298	0.195
4	0.211	0.365	0.310	0.000	0.205	0.378	0.162	0.006	0.076	0.174
5	0.066	0.061	0.327	0.058	0.000	0.196	0.039	0.017	0.275	0.179
6	0.241	0.330	0.347	0.054	0.030	0.000	0.053	0.068	0.073	0.123
7	0.105	0.215	0.034	0.348	0.096	0.135	0.000	0.260	0.147	0.203
8	0.262	0.398	0.160	0.232	0.049	0.360	0.382	0.000	0.250	0.204
9	0.276	0.031	0.104	0.220	0.074	0.148	0.230	0.259	0.000	0.327
10	0.299	0.177	0.320	0.058	0.096	0.044	0.024	0.180	0.032	0.000

Table 5.2: Summary of Results Obtained from Solving the ILP and Comparison with OBS for the Ring Network. For OBS number of independent flows per link are shown. Load values are normalized to a single wavelength channel.

		ρ_{max_w}	Total no. of VOBs	No. VOBs per link			Load per link		
				Avg.	Min.	Max.	Avg.	Min.	Max.
VOB	Random	0.7	13	3.95	3	4	2.29	1.61	2.85
		0.75	16	3.95	3	4	2.31	1.59	2.66
	Uniform	0.7	23	4.95	4	5	2.34	2.24	2.43
		0.75	14	3.95	3	4	2.36	2.06	2.62
OBS	Random		-	12.5	10	15	2.24	1.69	2.96
	Uniform		-	12.5	10	15	2.34	1.87	2.81

value of the ρ_{max_w} in the interval where the average number of VOBs per link remains fixed.

In contrast to the case with random traffic, under the uniform traffic matrix a small change in the ρ_{max_w} causes a big jump in the total number of VOBs and also a change in the average number of VOBs per link. In fact, under the uniform traffic matrix all the demands are the same and therefore the play ground for the optimization and for clustering is not as big as that under the random traffic. For example, for the uniform traffic considered in this analysis the maximum number of flows per VOB per link is limited to 4 and 3 at ρ_{max_w}=0.7 and 0.75, respectively. That is, at ρ_{max_w}=0.7 a VOB could be loaded at most to $3 \times 0.187 = 0.561$ of the channel capacity, thus number of required VOBs to support the traffic demand at ρ_{max_w}=0.7 would be much larger than that at ρ_{max_w}=0.75.

5.1.2 NSFNET

The traffic matrix used for NSFNET topology is a measurement-based estimation of traffic in the NSFNET backbone as given in [Mukh 06]. The estimation presented in [Mukh 06]

Table 5.3: Traffic Matrix of NSFNET.

	0	1	2	3	4	5	6	7	8	9	10	11	12	13
0	0.00	0.08	0.03	0.01	0.06	0.00	0.02	0.07	0.01	0.01	0.09	0.03	0.06	0.01
1	0.21	0.00	0.18	0.09	0.17	0.08	0.12	0.46	0.03	0.06	0.24	0.31	0.23	0.16
2	0.03	0.14	0.00	0.14	0.03	0.11	0.03	0.26	0.03	0.01	0.15	0.02	0.06	0.04
3	0.02	0.02	0.04	0.00	0.01	0.00	0.00	0.01	0.01	0.01	0.04	0.04	0.02	0.01
4	0.37	0.48	0.06	0.01	0.00	0.01	0.03	0.19	0.07	0.05	0.22	0.35	0.06	0.04
5	0.01	0.05	0.01	0.02	0.01	0.00	0.01	0.01	0.00	0.01	0.02	0.01	0.02	0.00
6	0.11	0.19	0.31	0.01	0.07	0.02	0.00	0.34	0.06	0.07	0.46	0.28	0.49	0.07
7	0.04	0.70	0.63	0.03	0.08	0.01	0.29	0.00	0.13	0.10	0.27	0.21	0.27	0.06
8	0.25	0.06	0.11	0.02	0.07	0.02	0.07	0.18	0.00	0.12	0.33	0.44	0.19	0.14
9	0.01	0.13	0.03	0.01	0.07	0.03	0.01	0.17	0.02	0.00	0.11	0.08	0.04	0.04
10	0.03	0.11	0.17	0.02	0.03	0.04	0.06	0.11	0.06	0.07	0.00	0.18	0.11	0.10
11	0.09	0.39	0.06	0.04	0.13	0.02	0.05	0.17	0.12	0.09	0.63	0.00	0.20	0.08
12	0.24	0.68	0.16	0.07	0.27	0.09	0.10	0.27	0.09	0.00	0.39	0.41	0.00	0.19
13	0.12	0.17	0.06	0.02	0.03	0.00	0.01	0.07	0.35	0.11	0.21	0.24	0.16	0.00

shows the aggregate number of bytes between each pair of nodes in a 15-minutes interval as measured in 1992. We use these numbers as an approximate indication of relative intensities of demands between pairs of nodes in the network and accordingly scale the numbers in a way that the maximum element of the demand matrix is equal to 7 Gb/s. The resulting demand matrix is depicted in Table 5.3, where each value is normalized to 10 Gb/s.

In contrast to the ring topology, here the total number of possible paths that can be generated by the k-shortest path routing algorithm in the preprocessing phase is not a small number. Therefore, in order to evaluate possible impacts of total number of paths on results of optimization, we solve the ILP with four sets of VOB candidates $\mathbb{P}$, where each has a different size P. Taking into account that in the NSFNET with 14 nodes the set $\mathbb{P}$ should at least contain 182 paths, i.e. one path for each source-destination pair, we solve the ILP formulation for $P = 182, 364, 546, 728$, which correspond to 1, 2, 3 and 4 paths per source-destination pair, respectively. For solving the ILP in all the considered cases, we set $\rho_{max_w} = 0.7$. A summary of the results obtained through solving the corresponding ILPs are given in Table 5.4. Also, details of the solutions are given in Table A.5-A.8 in Appendix A.

First observe that, as expected, applying the clustering significantly reduces number of independent flows in the network as well as number of flows associated to the links. Specifically, the total number of VOBs in the network reduces with the number of VOB candidates, which is in direct relation with k, such that at $k=4$ the total number of VOBs is equal to 38, which is almost 79% lesser than that in OBS. For the same setting, the maximum number of independent flows per any link in the network reduces around 78%, i.e. from 18 to 4. In addition, even establishment of VOBs based on the set of paths obtained from the first shortest path routing, the case with $k=1$, considerably reduces both total number of independent flows and number of flows per link.

TKN-10-002

Page 28

Table 5.4: Summary of Results Obtained from Solving the ILP and Comparison with OBS for NSFNET. For OBS number of independent flows are shown instead of no. of VOBs. Load values are normalized to a single wavelength channel.

	k	Total no. of VOBs	No. VOBs per link			Load per link		
			Avg.	Min.	Max.	Avg.	Min.	Max.
VOB	1	81	4.45	2	12	1.11	0.16	2.33
	2	50	4.21	2	5	1.22	0.18	3.0
	3	40	3.71	3	4	1.20	0.31	2.71
	4	38	3.74	2	4	1.3	0.25	2.66
OBS		182	9.29	4	18	1.11	0.16	2.33

As for the impact of k on the optimization results, it is seen that at the beginning increasing k from 1 to 2 leads to a sharp reduction in the total number of VOBs as well as maximum number of VOBs per link. Nevertheless, beyond $k=2$ further improvements of the results through increasing k slows down. This is in fact because the optimum value of the objective function is approached. More specifically, the optimum value of the objective function is achieved at $k=3$ and further increasing of k will not improve the solution any further. Nevertheless, increasing k from 3 to 4 leads to the slightly lesser number of total VOBs in the network since it results in the selection of longer of VOBs by the solver. This is also reflected in the increased value of the average number of VOBs per link at $k=4$ as compared to that at $k=3$.

5.2 Performance Results

In order to quantify the performance of the VOB network explained in the last section we developed a simulation model of the network in OMNeT++. The simulation model can be set to work under both VOB and OBS. In either case, the just enough time (JET) protocol [Xion 00] is used for channel reservation in the network. Packets for each O-D flow are generated according to the Poisson process with deterministic packet size of 10 KB. The assumptions on the traffic are in line with the traffic analysis presented in [Rost 09]. For the ring network the arrival rates of the packets are set in a way that the average load generated for each flow is in agreement with the corresponding value in Table 5.1 for the random traffic scenario and is equal to 0.187 for the uniform traffic matrix. Similarly for the NSFNET scenario, the arrival rates are set according to load values given in Table 5.3. In case F = 1, length of the delay line is set in a way that it provides delay equal to transmission time of a single packet over the channel. For the sake of simplicity, in our simulations we assume the propagation delays in the network to be negligible. Additionally, in case of OBS, the shortest path routing is used for routing packets through the network.

Tables 5.5 and 5.6 present the results of simulating the ring network and the NSFNET, respectively. Shown in the tables are the average values of packet drop rate, throughput and access delay as well as the maximum value in the set of the average access delays of all the O-D flows for each scenario. The results are further compared with those obtained from the

simulation of the same network under OBS operation. For the ring network the results are also presented for the case $F = 1$.

First and foremost, we observe that the packet drop rate improves greatly when the VOB architecture is employed in comparison to OBS. Specifically, for the case that the maximum number of VOBs per link is equal to the available wavelength channels on the link the loss rate is completely suppressed and no instance of packet loss is observed during the long simulation periods.

In addition, as depicted in Tables 5.5 between one to two orders of magnitude reduction in the loss rate is seen even when number of wavelength channels are smaller than that of VOBs. In this case, the improvement in the loss rate becomes larger with the number of FDL buffers.

The elimination/reduction of the loss rate, which has been the first objective of designing the VOB architecture, gives rise to the improvement of the overall throughput of the network. For the considered ring network the throughput improvement is up to 13.57%, which is associated to the uniform traffic with ρ_{max_w}=0.75 and without FDL buffer. Also for the case of NSFNET around 1.77% increase in the overall network throughput is achieved. As observed, the improvements in the throughput for the NSFNET scenario as well as the ring network at F=1 is marginal. In fact, although employing the VOB results in a large reduction in the loss rate in these cases, this does not lead to a noticeable increase in the overall throughput since the packet loss rate in the network under OBS is in the order of 10^{-2}–10^{-3}. Another reason for the marginal improvements in the throughput of the NSFNET is that the network is not highly loaded.

Table 5.5 also includes the results achieved at different values of k, which in turn reflect impacts of routing of O-D flows on the performance of VOB architecture. For instance, in case k=1 the same routing is applied in VOB network as in OBS. From the table it is clear that routing of flows has an important role in the VOB architecture.

The cost of improvement in the packet loss rate and the network throughput is the access delay penalty that is introduced by the flow coordination in the VOB approach. Nevertheless, it is seen in Tables 5.5 and 5.6 that the delay penalty is negligible for all the investigated scenarios–taking into account that propagation delays in a typical metro/core network are in the range of 10s ms. For instance the average length of the links in NSFNET is 1081 km that leads to 5.4 ms propagation delay per hop, in average. The acceptable access delays indicate that the values of ρ_{max_w} are set properly in the VOB layout design phase.

TKN-10-002
Page 30

Table 5.5: Performance Evaluation Results for the Ring Network. Unless otherwise stated the VOB results are related to ρ_{max_w}=0.7. The average values are shown with 90% confidence level.

			Avg. Packet Drop Rate	Avg. Network Throughput (Mb/s)	Avg. Access Delay over all flows (μs)	Max Access Delay over all flows (μs)
Random	F=0	VOB	0	168645	12.3	52.7
			-	± 5.02	$\pm 6.5 \times 10^{-3}$	± 0.77
Traffic		OBS	9.4×10^{-2}	152763	1.7	2.98
			$\pm 2.4 \times 10^{-5}$	± 8.9	$\pm 3.7 \times 10^{-4}$	± 0.1
	F=0	VOB	3.6×10^{-2}	162287	6.2	12.2
			$\pm 2.4 \times 10^{-5}$	± 26.2	$\pm 7.5 \times 10^{-3}$	± 2.2
Uniform		VOB ρ_{max_w}=0.75	0	168657	21.1	62.7
			$-$	± 32	$\pm 4.9 \times 10^{-2}$	± 11.5
		OBS	1.2×10^{-1}	148250	1.2	1.8
			$\pm 6.6 \times 10^{-5}$	± 25.2	$\pm 7.5 \times 10^{-3}$	± 1.3
Traffic	F=1	VOB	5.9×10^{-5}	168561	6.6	12.6
			$\pm 6.4 \times 10^{-7}$	± 7.1	$\pm 1.6 \times 10^{-3}$	± 2.3
		OBS	3.8×10^{-3}	167732	2.1	4.2
			$\pm 1.7 \times 10^{-5}$	± 30.3	$\pm 3.5 \times 10^{-3}$	$\pm 6.5 \times 10^{-1}$

Table 5.6: Performance Evaluation Results for the NSFNET. The average values are shown with 90% confidence level.

	Avg. Packet Drop Rate	Avg. Network Throughput (Mb/s)	Avg. Access Delay over all flows (μs)	Max Access Delay over all flows (μs)
VOB (k=1)	1.08×10^{-2} $\pm 2.42 \times 10^{-5}$	217022 ± 27.19	3.74 $\pm 4.9 \times 10^{-3}$	20.11 ± 0.16
VOB (k=2)	6.6×10^{-3} $\pm 7.47 \times 10^{-6}$	217947 ± 27.52	5.86 $\pm 4.5 \times 10^{-3}$	43.69 ± 0.73
VOB (k=3)	0 -	219400 ± 28.18	6.75 $\pm 8.8 \times 10^{-3}$	49.65 ± 0.92
VOB (k=4)	0 -	219400 ± 28.19	6.93 $\pm 1 \times 10^{-2}$	42.07 ± 0.43
OBS	1.75×10^{-2} $\pm 2.01 \times 10^{-5}$	215567 ± 17.4	2.18 $\pm 1.7 \times 10^{-3}$	9.41 $\pm 2.7 \times 10^{-2}$

Chapter 6

Related Works

Although there is a large number of publications on contention resolution issue of OBS networks, only few of them consider the proactive measures to reduce packet collisions rate. In this section we outline the most relevant approaches and compare them with VOB.

Authors in [Guma 04] present a new packet-based optical transport architecture based on light trail (LT), which is a generalized form of the light path (optical circuit) where intermediate nodes along the path of the circuit may also inject traffic into that. Therefore, a LT could also be considered as an optical bus that facilitates traffic grooming in the network. Our approach is essentially different from the LT. Specifically, in the LT approach the whole capacity of a wavelength channel must be dedicated to each LT on any link in the network being part of that LT and there is no switching in the intermediate nodes. That is, the LT approach allows only for intra-wavelength multiplexing. With the VOB approach, however, a single wavelength on a link may be shared by all the VOBs on that link, i.e., both intra- and inter-wavelength multiplexing are realized. On the other hand, in order to transmit any packet using LT one needs to establish a LT in advance, whereas in the VOB establishing a virtual bus can take place in the background while transmission of packets are in progress.

In [Li 03] authors present a proactive burst scheduling algorithm aiming at reducing the collision rate in the network. In this approach, every node injects its local packets into the network in a way that they do not overlap in time with each other if the packets are supposed to traverse the same path. Our approach based on VOB differs from proactive burst scheduling, in that the latter one only does a local coordination at every ingress node through implementing a new MAC protocol assuming that routings of the O-D flows are already fixed. In the VOB-based approach, however, a network-wide traffic engineering is applied, which also involves finding appropriate paths for the flows to reduce the potential of collisions in the network.

Dual bus optical ring (DBORN) is an architecture for optical metro transport networks that has studied in [Hu 05]. A metro network based on DBORN is composed of two WDM rings, where one is used as the working ring and the other one as the back up and WDM channels on each link are divided into upstream and downstream channels. All nodes attached to the ring are passive except one node that is called hub and is the only node who can transmit the traffic over the downstream channels and receives or removes traffic over the upstream channels. All the passive nodes have access to the upstream channels using an optical carrier sense multiple access with collision avoidance (CSMA/CA) MAC protocol. In

order that node i transmit a data packet to node j, where i and j are both attached to the ring, node i has to first transmit the packet to the hub over one of the upstream channels and then the hub node would forward the packet to node j on one of the downstream nodes. In DBORN both the transmission and the packet processing of the whole network are limited by those of the hub node. Also, the resources in the network are not utilized efficiently since for example to transmit a packet form a given node to its adjacent node the packet has to travel the whole circumference of the ring network first. In contrast to DBORN, VOB can achieve a high network utilization since source-destination pairs communicate directly and without using a hub. In addition, DBORN is a ring-based approach and is not extended to an arbitrary meshed topology, whereas VOB architecture can be applied to any meshed topology.

Authors in [Widj 04] present time-domain wavelength interleaved networking (TWIN) as a new optical transport architecture. TWIN consists of smart edge nodes that are equipped with ultra-fast tunable lasers and passive fixed-routing optical core nodes. A unique wavelength is assigned to each destination node in the network, which by the way serves as the address of that node. In order to transmit a packet from node i to node j, the node i has to tune its tunable laser to the wavelength associated to node j for the duration of the packet transmission. All the passive intermediate nodes are configured in advance to guide incoming packets towards their destinations based on the wavelength channel that the packets are arriving on. In this way, a multipoint-to-point tree is formed to every egress node in the network. The key design issue of the TWIN architecture is to devise a scheduler that can handle a collision-free transmission of packets on a given destination tree. Designing an appropriate scheduling algorithm that can work efficiently under highly dynamic traffic is a challenging issue. In fact a fixed scheduling for all nodes of a tree has to be calculated before any packet transmission can take place on that tree. This is, however, not required in VOB architecture that instead of trees uses busses, which are much easier to coordinate. Additionally, the number of wavelength channels in TWIN must always be at least equal to the number of nodes in the network, whereas in VOB there is no constraint on the required number of wavelengths in the network.

TKN-10-002
Page 34

Chapter 7

Conclusion and Future Work

We presented VOB as a new architecture for dynamic sub-wavelength allocation of bandwidth in optical transport networks. The VOB is based on establishing a coordination among a set of ingress nodes in the network in a way that no collision occurs among packets belonging to these nodes. We formulated design of a VOB-based network, which consists of grouping all aggregate flows into VOBs, as an ILP formulation with the objective of minimizing inter-VOB collisions.

Also, two design examples are presented to quantify the merits of VOB network architecture. Our numerical results demonstrated that this approach can greatly alleviate the contention problem that is central to the design of OBS networks. In one of the design examples we presented a bidirectional ring network with 10 nodes and 4 wavelength channels–10 Gb/s each–in each direction. The presented network achieves 168.6 Gb/s throughput and has zero packet loss inside the network. The same network under OBS operation has 148.2 Gb/s throughput—13.5% less–and suffers from 12% packet loss rate. In addition, similar performance improvements are demonstrated for the NSFNET backbone with 14 nodes.

There are some issues that can be considered as the future direction to the presented architecture. Among others, an appropriate signaling scheme has to be developed for setting up VOBs inside the network. Also, network layout reconfiguration triggered by changes in demand matrix is an issue that deserves further study.

Appendix A

Results of Solving ILP for Design Examples

Table A.1: Results Obtained from Solving the ILP for the Ring Network with Random Traffic Matrix at ρ_{max_w}=0.7

VOB id	Route	Associated O-D Flows
1	$(0 \rightarrow 9 \rightarrow 8 \rightarrow 7 \rightarrow 6)$	$(0,6), (0,9), (7,6), (9,7), (9,8)$
2	$(0 \rightarrow 1 \rightarrow 2 \rightarrow 3 \rightarrow 4 \rightarrow 5 \rightarrow 6 \rightarrow 7 \rightarrow 8)$	$(0,1), (0,2), (0,4), (0,7), (1,6), (2,6),$ $(4,8), (6,8), (7,8)$
3	$(1 \rightarrow 2 \rightarrow 3 \rightarrow 4 \rightarrow 5 \rightarrow 6 \rightarrow 7 \rightarrow 8 \rightarrow 9 \rightarrow 0)$	$(1,2), (1,4), (2,5), (3,7), (3,8), (4,5),$ $(5,8), (6,9), (7,9), (8,0), (9,0)$
4	$(1 \rightarrow 0 \rightarrow 9 \rightarrow 8 \rightarrow 7 \rightarrow 6 \rightarrow 5 \rightarrow 4 \rightarrow 3 \rightarrow 2)$	$(0,5), (1,7), (1,9), (4,2), (6,2), (7,2),$ $(7,4), (8,2), (8,4), (9,4), (9,6)$
5	$(2 \rightarrow 1)$	$(2,1)$
6	$(3 \rightarrow 4 \rightarrow 5 \rightarrow 6 \rightarrow 7 \rightarrow 8 \rightarrow 9 \rightarrow 0 \rightarrow 1)$	$(3,4), (3,5), (4,1), (4,9), (5,0), (6,1),$ $(9,1)$
7	$(5 \rightarrow 4 \rightarrow 3 \rightarrow 2 \rightarrow 1 \rightarrow 0 \rightarrow 9 \rightarrow 8)$	$(0,8), (1,8), (2,8), (5,1), (5,2)$
8	$(6 \rightarrow 5 \rightarrow 4 \rightarrow 3 \rightarrow 2 \rightarrow 1 \rightarrow 0 \rightarrow 9)$	$(2,0), (2,9), (3,2), (3,9), (4,0),$ $(4,3), (5,9), (6,3), (6,4)$
9	$(7 \rightarrow 8 \rightarrow 9 \rightarrow 0 \rightarrow 1 \rightarrow 2 \rightarrow 3)$	$(0,3), (1,3), (7,0), (7,1), (8,1)$
10	$(8 \rightarrow 7 \rightarrow 6 \rightarrow 5 \rightarrow 4 \rightarrow 3 \rightarrow 2 \rightarrow 1 \rightarrow 0)$	$(1,0), (3,0), (3,1), (5,3), (5,4), (6,0),$ $(7,3), (8,3), (8,6)$
11	$(8 \rightarrow 7 \rightarrow 6 \rightarrow 5)$	$(6,5), (7,5), (8,5), (8,7)$
12	$(8 \rightarrow 9)$	$(8,9)$
13	$(9 \rightarrow 0 \rightarrow 1 \rightarrow 2 \rightarrow 3 \rightarrow 4 \rightarrow 5 \rightarrow 6 \rightarrow 7)$	$(1,5), (2,3), (2,4), (2,7), (3,6), (4,6),$ $(4,7), (5,6), (5,7), (6,7), (9,2), (9,3),$ $(9,5)$

Table A.2: Results Obtained from Solving the ILP for the
Ring Network with Random Traffic Matrix at ρ_{max_w}=0.75

VOB id	Route	Associated O-D Flows
1	$(0 \to 9 \to 8 \to 7 \to 6 \to 5 \to 4)$	$(0,8),(6,4),(7,5),(8,5),$ $(9,4),(9,5)$
2	$(0 \to 1 \to 2 \to 3 \to 4 \to 5)$	$(0,1),(0,4),(1,2),(1,5),$ $(2,5),(4,5)$
3	$(1 \to 0 \to 9)$	$(0,9),(1,0),(1,9)$
4	$(1 \to 2 \to 3 \to 4 \to 5 \to 6 \to 7 \to 8 \to 9)$	$(1,4),(2,3),(2,4),(3,6),$ $(3,9),(4,9),(5,9),(6,9)$
5	$(2 \to 1 \to 0)$	$(2,0)$
6	$(3 \to 2 \to 1 \to 0 \to 9 \to 8 \to 7)$	$(0,7),(2,8),(2,9),(3,0),$ $(3,2),(8,7),(9,7)$
7	$(3 \to 4 \to 5 \to 6 \to 7 \to 8)$	$(3,4),(3,5),(3,8),(4,7),$ $(4,8),(5,7),(5,8),(7,8)$
8	$(4 \to 3 \to 2 \to 1)$	$(2,1),(3,1),(4,2)$
9	$(5 \to 4 \to 3 \to 2 \to 1 \to 0 \to 9 \to 8 \to 7 \to 6)$	$(0,6),(1,6),(1,8),(4,0),$ $(4,1),(4,6),(5,0),(5,1),$ $(5,4),(8,6),(9,8)$
10	$(6 \to 7 \to 8 \to 9 \to 0 \to 1 \to 2 \to 3)$	$(0,3),(1,3),(6,0),(6,1),$ $(6,2),(6,8),(7,9),(8,2),$ $(9,3)$
11	$(6 \to 5)$	$(6,5)$
12	$(7 \to 8 \to 9 \to 0 \to 1)$	$(7,0),(7,1),(8,1)$
13	$(7 \to 6 \to 5 \to 4 \to 3 \to 2)$	$(5,2),(7,2),(7,3)$
14	$(8 \to 9 \to 0)$	$(8,0),(8,9),(9,0)$
15	$(9 \to 8 \to 7 \to 6 \to 5 \to 4 \to 3)$	$(4,3),(5,3),(6,3),(7,4)$ $(7,6),(8,3),(8,4),(9,6)$
16	$(9 \to 0 \to 1 \to 2 \to 3 \to 4 \to 5 \to 6 \to 7)$	$(0,2),(0,5),(1,7),(2,6),$ $(2,7),(3,7),(5,6),(6,7),$ $(9,1),(9,2)$

Table A.3: Results Obtained from Solving the ILP for the
Ring Network with Uniform Traffic Matrix at ρ_{max_w}=0.7

VOB id	Route	Associated O-D Flows
1	$(0 \to 1 \to 2 \to 3 \to 4 \to 5)$	$(0,4),(0,5),(2,3),(3,5),(4,5)$
2	$(1 \to 2 \to 3 \to 4 \to 5)$	$(1,2),(1,5),(2,4),(2,5)$
3	$(1 \to 0 \to 9 \to 8 \to 7 \to 6)$	$(0,6),(0,7),(1,0),(1,7)$
4	$(1 \to 2 \to 3 \to 4 \to 5 \to 6)$	$(1,3),(1,4),(1,6),(3,6),(5,6)$
		Continued on next page

Table A.3 – continued from previous page

VOB id	Route	Associated O-D Flows
5	$(2 \to 3 \to 4 \to 5 \to 6 \to 7)$	$(2,6),(2,7),(3,7)$
6	$(2 \to 1 \to 0 \to 9 \to 8)$	$(0,8),(1,8),(2,9)$
7	$(3 \to 4)$	$(3,4)$
8	$(3 \to 2 \to 1 \to 0 \to 9 \to 8)$	$(1,9),(2,8),(3,1),(3,8)$
9	$(4 \to 3 \to 2 \to 1 \to 0)$	$(3,0),(4,0),(4,3)$
10	$(4 \to 5 \to 6 \to 7 \to 8)$	$(4,6),(4,7),(4,8),(6,8),(7,8)$
11	$(4 \to 3 \to 2 \to 1 \to 0 \to 9)$	$(0,9),(2,0),(3,9),(4,2),(4,9)$
12	$(5 \to 6 \to 7 \to 8 \to 9 \to 0)$	$(5,0),(5,7),(6,0),(7,9),(9,0)$
13	$(5 \to 4 \to 3 \to 2 \to 1)$	$(2,1),(4,1),(5,1)$
14	$(5 \to 6 \to 7 \to 8 \to 9)$	$(5,8),(5,9),(6,9)$
15	$(6 \to 7 \to 8 \to 9 \to 0 \to 1)$	$(6,1),(6,7),(7,1),(8,9),(9,1)$
16	$(6 \to 5 \to 4 \to 3 \to 2)$	$(3,2),(5,2),(5,3),(6,2)$
17	$(7 \to 8 \to 9 \to 0 \to 1 \to 2)$	$(0,2),(7,0),(7,2),(8,2)$
18	$(8 \to 9 \to 0 \to 1)$	$(0,1),(8,0),(8,1)$
19	$(8 \to 7 \to 6 \to 5 \to 4 \to 3)$	$(6,3),(7,3),(8,3),(8,6),(8,7)$
20	$(8 \to 7 \to 6 \to 5 \to 4)$	$(7,4),(8,4),(8,5)$
21	$(9 \to 0 \to 1 \to 2 \to 3)$	$(0,3),(9,2),(9,3)$
22	$(9 \to 8 \to 7 \to 6 \to 5 \to 4)$	$(5,4),(6,4),(7,5),(7,6),(9,4),(9,7),(9,8)$
23	$(9 \to 8 \to 7 \to 6 \to 5)$	$(6,5),(9,5),(9,6)$

Table A.4: Results Obtained from Solving the ILP for the
Ring Network with Uniform Traffic Matrix at ρ_{max_w}=0.75

VOB id	Route	Associated O-D Flows
1	$(1 \to 0 \to 9 \to 8 \to 7 \to 6 \to 5 \to 4)$	$(1,0),(1,7),(1,8),(1,9),$ $(5,4),(6,4),(7,6),(8,4),$ $(9,4),(9,5)$
2	$(1 \to 2 \to 3 \to 4 \to 5 \to 6 \to 7 \to 8 \to 9)$	$(1,3),(1,4),(1,5),(2,6),$ $(3,7),(5,8),(5,9),(6,9),$ $(7,9)$
3	$(3 \to 4)$	$(3,4)$
4	$(3 \to 4 \to 5 \to 6)$	$(3,5),(3,6)$
5	$(4 \to 5 \to 6 \to 7 \to 8 \to 9 \to 0)$	$(4,5),(4,8),(4,9),(5,0),$ $(6,0),(8,0)$
6	$(4 \to 3 \to 2 \to 1 \to 0 \to 9 \to 8 \to 7 \to 6)$	$(0,6),(1,6),(2,1),(2,8),$ $(3,0),(3,2),(4,0),(4,2),$ $(4,3),(8,6),(9,6)$
7	$(5 \to 4 \to 3 \to 2 \to 1)$	$(3,1),(4,1),(5,1),(5,2),$ $(5,3)$
		Continued on next page

Table A.4 – continued from previous page

VOB id	Route	Associated O-D Flows
8	$(6 \to 7 \to 8 \to 9 \to 0 \to 1 \to 2 \to 3)$	$(1,2),(6,7),(7,0),(8,1),$ $(8,2),(8,3)$
9	$(6 \to 5 \to 4 \to 3 \to 2 \to 1 \to 0 \to 9 \to 8 \to 7)$	$(0,7),(2,7),(2,9),(3,9),$ $(6,1),(6,2),(6,3),(6,5),$ $(8,7),(9,7),(9,8)$
10	$(7 \to 6 \to 5 \to 4 \to 3 \to 2 \to 1 \to 0 \to 9 \to 8)$	$(0,8),(0,9),(2,0),(3,8)$ $(7,1),(7,2),(7,3),(7,4)$
11	$(8 \to 7 \to 6 \to 5)$	$(7,5),(8,5)$
12	$(8 \to 9)$	$(8,9)$
13	$(9 \to 0 \to 1 \to 2 \to 3)$	$(0,3),(2,3),(9,1),(9,2),$ $(9,3)$
14	$(9 \to 0 \to 1 \to 2 \to 3 \to 4 \to 5 \to 6 \to 7 \to 8)$	$(0,1),(0,2),(0,4),(0,5),$ $(2,4),(4,7),(5,6),(2,5),$ $(4,6),(5,7),(6,8),(7,8),$ $(9,0)$

Table A.5: Results Obtained from Solving the ILP for NSFNET with $k=1$.

VOB id	Route	Associated O-D Flows
1	$(0 \to 7 \to 6 \to 4)$	$(0,4),(0,6),(0,7),(6,4),(7,4),(7,6)$
2	$(0 \to 7 \to 8 \to 9)$	$(0,8),(0,9),(7,8),(7,9),(8,9)$
3	$(0 \to 1 \to 3 \to 10)$	$(0,1),(0,3),(0,10),(1,3),(1,10),(3,10)$
4	$(0 \to 7 \to 8 \to 11)$	$(0,11),(7,11),(8,11)$
5	$(0 \to 2 \to 5 \to 12)$	$(0,2),(0,5),(0,12),(2,5),(2,12),(5,12)$
6	$(0 \to 7 \to 8 \to 13)$	$(0,13),(7,13),(8,13)$
7	$(1 \to 3 \to 4)$	$(1,4),(3,4)$
8	$(1 \to 0 \to 7 \to 6)$	$(1,6),(1,7)$
9	$(1 \to 0 \to 7 \to 8)$	$(1,8)$
10	$(1 \to 2 \to 5 \to 9)$	$(1,2),(1,5),(1,9),(2,9),(5,9)$
11	$(1 \to 3 \to 10 \to 11)$	$(1,11),(3,11),(10,11)$
12	$(1 \to 2 \to 5 \to 12)$	$(1,12)$
13	$(1 \to 3 \to 10 \to 13)$	$(1,13),(3,13),(10,13)$
14	$(2 \to 5 \to 4)$	$(2,4),(5,4)$
15	$(2 \to 0 \to 7 \to 6)$	$(2,0),(2,6),(2,7)$
16	$(2 \to 0 \to 7 \to 8)$	$(2,8)$
17	$(2 \to 1 \to 3 \to 10)$	$(2,1),(2,3),(2,10)$
18	$(2 \to 5 \to 12 \to 11)$	$(2,11),(5,11),(12,11)$
19	$(2 \to 5 \to 12 \to 13)$	$(2,13),(5,13),(12,13)$
20	$(3 \to 4 \to 6 \to 7)$	$(3,6),(3,7),(4,6),(4,7),(6,7)$
		Continued on next page

Table A.5 – continued from previous page

VOB id	Route	Associated O-D Flows
21	$(3 \rightarrow 10 \rightarrow 13 \rightarrow 8)$	$(3,8),(10,8),(13,8)$
22	$(3 \rightarrow 4 \rightarrow 5 \rightarrow 9)$	$(3,5),(3,9),(4,5),(4,9)$
23	$(3 \rightarrow 10 \rightarrow 13 \rightarrow 12)$	$(3,12),(10,12),(13,12)$
24	$(4 \rightarrow 3 \rightarrow 1 \rightarrow 0)$	$(1,0),(3,0),(3,1),(4,0),(4,3)$
25	$(4 \rightarrow 3 \rightarrow 1)$	$(4,1)$
26	$(4 \rightarrow 6 \rightarrow 7 \rightarrow 8)$	$(4,8),(6,8)$
27	$(4 \rightarrow 3 \rightarrow 10 \rightarrow 11)$	$(4,10),(4,11)$
28	$(4 \rightarrow 3 \rightarrow 10 \rightarrow 13)$	$(4,13)$
29	$(5 \rightarrow 4 \rightarrow 6 \rightarrow 7)$	$(5,6),(5,7)$
30	$(5 \rightarrow 9 \rightarrow 8)$	$(5,8),(9,8)$
31	$(5 \rightarrow 12 \rightarrow 13 \rightarrow 10)$	$(5,10),(12,10),(13,10)$
32	$(6 \rightarrow 7 \rightarrow 0 \rightarrow 1)$	$(6,0),(6,1),(7,0)$
33	$(6 \rightarrow 4 \rightarrow 5 \rightarrow 2)$	$(4,2),(5,2),(6,2),(6,5)$
34	$(6 \rightarrow 7 \rightarrow 8 \rightarrow 9)$	$(6,9)$
35	$(6 \rightarrow 4 \rightarrow 3 \rightarrow 10)$	$(6,3),(6,10)$
36	$(6 \rightarrow 7 \rightarrow 8 \rightarrow 11)$	$(6,11)$
37	$(6 \rightarrow 4 \rightarrow 5 \rightarrow 12)$	$(4,12),(6,12)$
38	$(6 \rightarrow 7 \rightarrow 8 \rightarrow 13)$	$(6,13)$
39	$(7 \rightarrow 0 \rightarrow 1)$	$(7,1)$
40	$(7 \rightarrow 0 \rightarrow 2)$	$(7,2)$
41	$(7 \rightarrow 0 \rightarrow 1 \rightarrow 3)$	$(7,3)$
42	$(7 \rightarrow 8 \rightarrow 9 \rightarrow 5)$	$(7,5),(8,5),(9,5)$
43	$(7 \rightarrow 8 \rightarrow 13 \rightarrow 10)$	$(7,10)$
44	$(7 \rightarrow 8 \rightarrow 13 \rightarrow 12)$	$(7,12),(8,12)$
45	$(8 \rightarrow 7 \rightarrow 0 \rightarrow 1)$	$(8,0),(8,1),(8,7)$
46	$(8 \rightarrow 7 \rightarrow 0 \rightarrow 2)$	$(8,2)$
47	$(8 \rightarrow 13 \rightarrow 10 \rightarrow 3)$	$(8,3),(8,10),(10,3),(13,3)$
48	$(8 \rightarrow 7 \rightarrow 6 \rightarrow 4)$	$(8,4),(8,6)$
49	$(9 \rightarrow 8 \rightarrow 7 \rightarrow 0)$	$(9,0),(9,7)$
50	$(9 \rightarrow 5 \rightarrow 2 \rightarrow 1)$	$(5,1),(9,1),(9,2)$
51	$(9 \rightarrow 5 \rightarrow 4 \rightarrow 3)$	$(5,3),(9,3),(9,4)$
52	$(9 \rightarrow 8 \rightarrow 7 \rightarrow 6)$	$(9,6)$
53	$(9 \rightarrow 8 \rightarrow 13 \rightarrow 10)$	$(9,10),(9,13)$
54	$(9 \rightarrow 8 \rightarrow 11)$	$(9,11)$
55	$(9 \rightarrow 5 \rightarrow 12)$	$(9,12)$
56	$(10 \rightarrow 3 \rightarrow 1 \rightarrow 0)$	$(10,0),(10,1)$
57	$(10 \rightarrow 3 \rightarrow 1 \rightarrow 2)$	$(3,2),(10,2)$
58	$(10 \rightarrow 11 \rightarrow 12 \rightarrow 5)$	$(10,5),(11,5),(11,12),(12,5)$
59	$(10 \rightarrow 3 \rightarrow 4 \rightarrow 6)$	$(10,4),(10,6)$
60	$(10 \rightarrow 13 \rightarrow 8 \rightarrow 7)$	$(10,7),(13,7)$
61	$(10 \rightarrow 13 \rightarrow 8 \rightarrow 9)$	$(10,9),(13,9)$
62	$(11 \rightarrow 8 \rightarrow 7 \rightarrow 0)$	$(11,0),(11,7),(11,8)$
		Continued on next page

Table A.5 – continued from previous page

VOB id	Route	Associated O-D Flows
63	$(11 \to 10 \to 3 \to 1)$	$(11,1),(11,3)$
64	$(11 \to 12 \to 5 \to 2)$	$(11,2),(12,2)$
65	$(11 \to 10 \to 3 \to 4)$	$(11,4)$
66	$(11 \to 8 \to 7 \to 6)$	$(11,6)$
67	$(11 \to 8 \to 9)$	$(11,9)$
68	$(11 \to 10)$	$(11,10)$
69	$(11 \to 12 \to 13)$	$(11,13)$
70	$(12 \to 5 \to 2 \to 0)$	$(5,0),(12,0)$
71	$(12 \to 5 \to 2 \to 1)$	$(12,1)$
72	$(12 \to 13 \to 10 \to 3)$	$(12,3)$
73	$(12 \to 5 \to 4 \to 6)$	$(12,4),(12,6)$
74	$(12 \to 13 \to 8 \to 7)$	$(12,7),(12,8)$
75	$(12 \to 5 \to 9)$	$(12,9)$
76	$(13 \to 8 \to 7 \to 0)$	$(13,0)$
77	$(13 \to 10 \to 3 \to 1)$	$(13,1)$
78	$(13 \to 12 \to 5 \to 2)$	$(13,2),(13,5)$
79	$(13 \to 10 \to 3 \to 4)$	$(13,4)$
80	$(13 \to 8 \to 7 \to 6)$	$(13,6)$
81	$(13 \to 12 \to 11)$	$(13,11)$

Table A.6: Results Obtained from Solving the ILP for NSFNET with k=2.

VOB id	Route	Associated O-D Flows
1	$(0 \to 1 \to 3 \to 4 \to 6 \to 7)$	$(0,4),(1,4),(1,6),(3,7),(4,7),(6,7)$
2	$(0 \to 2 \to 5 \to 9 \to 8)$	$(0,5),(0,9),(2,8),(2,9),(5,8),$ $(5,9),(9,8)$
3	$(1 \to 2)$	$(1,2)$
4	$(1 \to 0 \to 7 \to 8 \to 13 \to 10)$	$(0,8),(0,13),(1,7),(1,8),$ $(1,13),(7,8),(7,10),(7,13),$ $(8,13),(13,10)$
5	$(1 \to 0 \to 7 \to 8 \to 11)$	$(0,11),(1,11),(7,11)$
6	$(1 \to 0 \to 2 \to 5 \to 12)$	$(0,2),(0,12),(1,12),(2,12)$
7	$(2 \to 1)$	$(2,1)$
8	$(2 \to 1 \to 3 \to 4 \to 5)$	$(1,3),(1,5),(2,4),(3,5),(4,5)$
9	$(2 \to 0 \to 7)$	$(2,7)$
10	$(2 \to 0 \to 1 \to 3 \to 10)$	$(0,3),(0,10),(1,10),(2,0),(2,10)$
11	$(2 \to 5 \to 9 \to 8 \to 11)$	$(2,11),(5,11),(8,11),(9,11)$
12	$(2 \to 5 \to 9 \to 8 \to 13 \to 12)$	$(2,13),(5,13),(8,12),(9,12),$ $(9,13),(13,12)$
		Continued on next page

Table A.6 – continued from previous page

VOB id	Route	Associated O-D Flows
13	$(3 \rightarrow 10 \rightarrow 13 \rightarrow 8)$	$(3,8),(10,8),(13,8)$
14	$(3 \rightarrow 1 \rightarrow 2 \rightarrow 5 \rightarrow 9)$	$(1,9),(2,5),(3,9)$
15	$(3 \rightarrow 10 \rightarrow 11 \rightarrow 12 \rightarrow 13)$	$(3,10),(3,12),(3,13),(10,11),(11,13)$
16	$(4 \rightarrow 5 \rightarrow 2 \rightarrow 0 \rightarrow 7 \rightarrow 6)$	$(0,6),(0,7),(2,6),(4,2),$
		$(4,6),(5,6),(5,7)$
17	$(4 \rightarrow 5 \rightarrow 12 \rightarrow 13 \rightarrow 10)$	$(4,12),(4,13),(5,10),(12,10)$
18	$(5 \rightarrow 12)$	$(5,12)$
19	$(6 \rightarrow 7 \rightarrow 0 \rightarrow 2)$	$(6,2),(7,0)$
20	$(6 \rightarrow 4 \rightarrow 3 \rightarrow 1 \rightarrow 0)$	$(1,0),(4,0),(6,0),(6,1)$
21	$(6 \rightarrow 4 \rightarrow 3 \rightarrow 10 \rightarrow 11)$	$(3,11),(4,11),(6,11)$
22	$(6 \rightarrow 7 \rightarrow 8 \rightarrow 13 \rightarrow 12)$	$(6,12),(6,13)$
23	$(6 \rightarrow 4 \rightarrow 3 \rightarrow 10)$	$(4,3),(4,10),(6,10)$
24	$(7 \rightarrow 0 \rightarrow 1)$	$(7,1)$
25	$(7 \rightarrow 6 \rightarrow 4 \rightarrow 3)$	$(6,3),(6,4),(7,3),(7,4)$
26	$(7 \rightarrow 6 \rightarrow 4 \rightarrow 5 \rightarrow 9 \rightarrow 8)$	$(4,8),(4,9),(6,5),(6,8),$
		$(6,9),(7,5),(7,6),(7,9)$
27	$(7 \rightarrow 8 \rightarrow 13 \rightarrow 12)$	$(7,12)$
28	$(8 \rightarrow 9 \rightarrow 5 \rightarrow 4 \rightarrow 6)$	$(8,4),(8,5),(9,4),(9,6)$
29	$(9 \rightarrow 5 \rightarrow 2 \rightarrow 0 \rightarrow 1)$	$(5,0),(9,0),(9,1),(9,2),(9,5)$
30	$(9 \rightarrow 5 \rightarrow 2 \rightarrow 1 \rightarrow 3)$	$(2,3),(9,3)$
31	$(9 \rightarrow 5 \rightarrow 4 \rightarrow 6 \rightarrow 7)$	$(9,7)$
32	$(9 \rightarrow 8 \rightarrow 11 \rightarrow 10)$	$(8,10),(9,10)$
33	$(10 \rightarrow 3 \rightarrow 1 \rightarrow 2 \rightarrow 0)$	$(3,0),(3,2),(10,0),(10,2)$
34	$(10 \rightarrow 3 \rightarrow 4 \rightarrow 5 \rightarrow 2 \rightarrow 1)$	$(3,4),(4,1),(5,1),(5,2),(10,4),$
		$(10,5)$
35	$(10 \rightarrow 13 \rightarrow 12 \rightarrow 5 \rightarrow 4 \rightarrow 3)$	$(5,3),(5,4),(10,3),(10,13),(12,3),$
		$(12,4),(13,3),(13,4),(13,5)$
36	$(10 \rightarrow 11 \rightarrow 12 \rightarrow 5 \rightarrow 4)$	$(10,12),(11,4)$
37	$(10 \rightarrow 11 \rightarrow 8 \rightarrow 7)$	$(10,7),(11,7)$
38	$(10 \rightarrow 11 \rightarrow 8 \rightarrow 9)$	$(10,9),(11,8)$
39	$(11 \rightarrow 10 \rightarrow 3 \rightarrow 1)$	$(3,1),(10,1),(11,1)$
40	$(11 \rightarrow 12 \rightarrow 5)$	$(11,5),(11,12),(12,5)$
41	$(11 \rightarrow 12 \rightarrow 13)$	$(12,13)$
42	$(12 \rightarrow 5 \rightarrow 2 \rightarrow 1)$	$(12,1)$
43	$(12 \rightarrow 11 \rightarrow 8 \rightarrow 7 \rightarrow 0 \rightarrow 2)$	$(8,2),(11,0),(11,2),(12,0),(12,2)$
44	$(12 \rightarrow 11 \rightarrow 8 \rightarrow 7 \rightarrow 6)$	$(8,6),(8,7),(11,6),(12,6),$
		$(12,7),(12,8)$
45	$(12 \rightarrow 11 \rightarrow 8 \rightarrow 9)$	$(11,9),(12,9),(12,11)$
46	$(13 \rightarrow 8 \rightarrow 7 \rightarrow 0 \rightarrow 1)$	$(0,1),(8,0),(8,1),(13,0),(13,1)$
47	$(13 \rightarrow 8 \rightarrow 7 \rightarrow 0 \rightarrow 2)$	$(7,2),(13,2),(13,7)$
48	$(13 \rightarrow 8 \rightarrow 11 \rightarrow 10 \rightarrow 3)$	$(8,3),(11,3),(11,10),(13,11)$
49	$(13 \rightarrow 10 \rightarrow 3 \rightarrow 4 \rightarrow 6)$	$(3,6),(10,6),(13,6)$
		Continued on next page

Table A.6 – continued from previous page

VOB id	Route	Associated O-D Flows
50	$(13 \to 8 \to 9)$	$(8, 9), (13, 9)$

Table A.7: Results Obtained from Solving the ILP for NSFNET with k=3.

VOB id	Route	Associated O-D Flows
1	$(0 \to 2 \to 5 \to 4 \to 6)$	$(0, 2), (2, 4), (2, 6)$
2	$(0 \to 1 \to 3 \to 4 \to 6 \to 7)$	$(0, 1), (0, 3), (0, 4), (0, 6),$
		$(1, 3), (1, 6), (3, 7), (4, 7)$
3	$(0 \to 1 \to 3 \to 10 \to 11)$	$(0, 10), (1, 10), (1, 11), (3, 10)$
4	$(1 \to 0 \to 7 \to 8 \to 13 \to 10)$	$(1, 7), (1, 8), (1, 13), (7, 8),$
		$(7, 10), (7, 13), (13, 10)$
5	$(1 \to 2 \to 5 \to 12 \to 13 \to 10)$	$(1, 5), (1, 12), (2, 5), (2, 10), (5, 12),$
		$(5, 13), (12, 10)$
6	$(2 \to 1 \to 0)$	$(1, 0), (2, 0), (2, 1)$
7	$(2 \to 1 \to 3)$	$(2, 3)$
8	$(2 \to 0 \to 7 \to 8 \to 11)$	$(0, 7), (0, 11), (2, 11), (7, 11)$
9	$(2 \to 0 \to 7 \to 8 \to 13 \to 12)$	$(0, 8), (0, 12), (0, 13), (2, 8),$
		$(2, 12), (2, 13), (7, 12), (8, 12)$
10	$(3 \to 1 \to 2 \to 5 \to 9)$	$(1, 9), (2, 9), (3, 2), (3, 5)$
11	$(3 \to 10 \to 13 \to 8 \to 9)$	$(3, 8), (3, 9), (10, 9)$
12	$(3 \to 4 \to 5 \to 12 \to 11 \to 10)$	$(3, 11), (3, 12), (4, 11), (5, 10),$
		$(5, 11), (11, 10)$
13	$(4 \to 5 \to 2 \to 0)$	$(4, 0), (4, 2), (4, 5)$
14	$(4 \to 5 \to 9 \to 8)$	$(4, 8), (4, 9), (5, 8)$
15	$(6 \to 7 \to 0 \to 2 \to 5 \to 9)$	$(0, 5), (0, 9), (5, 9), (6, 0), (6, 2), (6, 5),$
		$(6, 9), (7, 0), (7, 5), (7, 9)$
16	$(6 \to 7 \to 8 \to 11 \to 12)$	$(6, 7), (6, 8), (6, 11), (11, 12)$
17	$(6 \to 4 \to 3 \to 10 \to 13)$	$(3, 13), (4, 3), (4, 10), (6, 3),$
		$(6, 10), (10, 13)$
18	$(6 \to 4 \to 5 \to 12 \to 13)$	$(4, 12), (4, 13), (6, 4), (6, 12),$
		$(6, 13), (12, 13)$
19	$(7 \to 0 \to 1 \to 3 \to 4)$	$(1, 4), (7, 1)$
20	$(7 \to 6 \to 4 \to 3 \to 1)$	$(3, 1), (4, 1), (6, 1), (7, 3), (7, 4)$
21	$(8 \to 13 \to 10 \to 3 \to 1 \to 0)$	$(3, 0), (8, 0), (8, 1), (8, 13), (10, 0),$
		$(13, 0), (13, 1)$
22	$(8 \to 11 \to 10 \to 3 \to 4 \to 6)$	$(3, 4), (3, 6), (4, 6), (8, 4), (8, 10),$
		$(11, 3), (11, 4), (11, 6)$
23	$(9 \to 5 \to 2 \to 1 \to 0)$	$(5, 1), (9, 0), (9, 1)$
24	$(9 \to 8 \to 13 \to 10 \to 3)$	$(8, 3), (9, 3), (9, 10), (9, 13),$
Continued on next page		

TKN-10-002

<div align="center">

Table A.7 – continued from previous page

</div>

VOB id	Route	Associated O-D Flows
		$(10,3),(13,3)$
25	$(9 \to 5 \to 4 \to 6)$	$(5,6),(9,4),(9,5),(9,6)$
26	$(9 \to 5 \to 2 \to 0 \to 7)$	$(2,7),(5,0),(5,7),(9,2),(9,7)$
27	$(9 \to 8)$	$(9,8)$
28	$(9 \to 8 \to 11 \to 12)$	$(8,11),(9,11),(9,12)$
29	$(10 \to 13 \to 12 \to 5 \to 4 \to 3)$	$(5,3),(5,4),(10,5),(13,4)$
30	$(10 \to 11 \to 12 \to 5 \to 4 \to 3)$	$(10,4),(10,11),(10,12),(12,3),$
		$(12,4),(12,5)$
31	$(10 \to 11 \to 8 \to 7 \to 6)$	$(8,6),(8,7),(10,6),(10,7),$
		$(10,8),(11,7)$
32	$(11 \to 12 \to 5 \to 2 \to 1)$	$(5,2),(11,5),(12,1)$
33	$(11 \to 10 \to 3 \to 1 \to 2)$	$(1,2),(10,1),(10,2),(11,1)$
34	$(11 \to 10 \to 13)$	$(11,13)$
35	$(12 \to 11 \to 8 \to 7 \to 0 \to 2)$	$(8,2),(11,0),(11,2),(12,0),$
		$(12,2),(12,8)$
36	$(12 \to 13 \to 8 \to 7 \to 6)$	$(7,6),(12,6),(12,7),(13,6)$
37	$(12 \to 11 \to 8 \to 9)$	$(8,9),(12,9),(12,11)$
38	$(13 \to 8 \to 7 \to 0 \to 2)$	$(7,2),(13,2),(13,7)$
39	$(13 \to 8 \to 9 \to 5)$	$(8,5),(13,5),(13,8),(13,9)$
40	$(13 \to 12 \to 11 \to 8 \to 9)$	$(11,8),(11,9),(13,11),(13,12)$

<div align="center">

Table A.8: Results Obtained from Solving the ILP for
NSFNET with k=4.

</div>

VOB id	Route	Associated O-D Flows
1	$(0 \to 1)$	$(0,1)$
2	$(0 \to 2 \to 5 \to 12 \to 13 \to 8)$	$(0,8),(0,12),(0,13),(2,8),(2,12),(2,13),$
		$(5,12),(5,13),(12,8),(12,13),(13,8)$
3	$(0 \to 7 \to 8 \to 9)$	$(0,7),(0,9),(7,9)$
4	$(1 \to 0 \to 7 \to 6 \to 4 \to 3)$	$(0,3),(0,4),(0,6),(1,4),$
		$(1,6),(6,3),(7,3)$
5	$(1 \to 0 \to 7 \to 8 \to 11 \to 10)$	$(0,10),(0,11),(1,7),(1,8),$
		$(7,10),(7,11)$
6	$(1 \to 3 \to 10 \to 13 \to 12)$	$(1,3),(1,12),(1,13),$
		$(3,10),(3,13)$
7	$(2 \to 0 \to 1 \to 3 \to 10)$	$(2,10)$
8	$(2 \to 1 \to 3 \to 10 \to 11)$	$(1,10),(1,11),(2,11),(3,11)$
9	$(3 \to 10 \to 13 \to 8 \to 7)$	$(3,7),(3,8),(10,7)$
10	$(3 \to 4 \to 5 \to 12 \to 13 \to 10)$	$(3,4),(3,12),(4,10),(4,12),(4,13),(5,10),$
		$(12,10)$
		Continued on next page

Table A.8 – continued from previous page

VOB id	Route	Associated O-D Flows
11	$(4 \rightarrow 6)$	$(4, 6)$
12	$(4 \rightarrow 5 \rightarrow 9 \rightarrow 8 \rightarrow 7)$	$(4, 7), (4, 8), (5, 8), (8, 7), (9, 7)$
13	$(4 \rightarrow 3 \rightarrow 1 \rightarrow 2 \rightarrow 5 \rightarrow 9)$	$(1, 9), (2, 9), (3, 1), (3, 5),$
		$(3, 9), (4, 1), (4, 2), (4, 9)$
14	$(5 \rightarrow 2 \rightarrow 0 \rightarrow 7 \rightarrow 6 \rightarrow 4)$	$(2, 0), (2, 4), (2, 6), (2, 7),$
		$(5, 4), (5, 6), (5, 7), (6, 4)$
15	$(6 \rightarrow 7 \rightarrow 0 \rightarrow 1 \rightarrow 2 \rightarrow 5)$	$(0, 2), (0, 5), (1, 2), (1, 5), (2, 5),$
		$(6, 0), (6, 1), (6, 2), (7, 5)$
16	$(6 \rightarrow 7 \rightarrow 0 \rightarrow 2 \rightarrow 5 \rightarrow 9)$	$(5, 9), (6, 7), (6, 9), (7, 2)$
17	$(6 \rightarrow 7 \rightarrow 8 \rightarrow 11 \rightarrow 10)$	$(6, 8), (6, 10)$
18	$(6 \rightarrow 7 \rightarrow 8 \rightarrow 11 \rightarrow 12)$	$(6, 11), (7, 8), (7, 12)$
19	$(7 \rightarrow 0 \rightarrow 2 \rightarrow 1)$	$(7, 1)$
20	$(7 \rightarrow 6 \rightarrow 4 \rightarrow 5 \rightarrow 12 \rightarrow 13)$	$(4, 5), (6, 5), (6, 12), (6, 13), (7, 6), (7, 13)$
21	$(8 \rightarrow 9 \rightarrow 5 \rightarrow 2 \rightarrow 1)$	$(2, 1), (5, 2), (8, 1), (8, 2), (8, 5),$
		$(8, 9), (9, 1), (9, 2), (9, 5)$
22	$(8 \rightarrow 9 \rightarrow 5 \rightarrow 4 \rightarrow 6)$	$(8, 6), (9, 4), (9, 6)$
23	$(8 \rightarrow 11 \rightarrow 12 \rightarrow 5 \rightarrow 9)$	$(8, 11), (8, 12), (11, 5), (11, 12), (12, 5), (12, 9)$
24	$(9 \rightarrow 5 \rightarrow 4 \rightarrow 3 \rightarrow 1 \rightarrow 0)$	$(4, 0), (5, 0), (5, 1), (5, 3), (9, 0)$
25	$(9 \rightarrow 8 \rightarrow 13 \rightarrow 10 \rightarrow 3 \rightarrow 4 \rightarrow 6)$	$(8, 3), (8, 10), (8, 13), (9, 3), (9, 10), (9, 13),$
		$(10, 3), (10, 6), (13, 6), (13, 10)$
26	$(9 \rightarrow 8)$	$(9, 8)$
27	$(9 \rightarrow 8 \rightarrow 13 \rightarrow 12 \rightarrow 11)$	$(9, 11), (9, 12), (12, 11), (13, 12)$
28	$(10 \rightarrow 13 \rightarrow 12 \rightarrow 5 \rightarrow 4 \rightarrow 3)$	$(4, 3), (10, 5), (10, 13), (12, 3),$
		$(12, 4), (13, 4), (13, 5)$
29	$(10 \rightarrow 13 \rightarrow 12 \rightarrow 5 \rightarrow 2 \rightarrow 1 \rightarrow 3)$	$(2, 3), (10, 1), (10, 2), (10, 12),$
		$(12, 2), (13, 1), (13, 2), (13, 3)$
30	$(10 \rightarrow 3 \rightarrow 4 \rightarrow 5 \rightarrow 12 \rightarrow 11)$	$(4, 11), (5, 11), (10, 4)$
31	$(10 \rightarrow 11 \rightarrow 8 \rightarrow 13)$	$(10, 11), (11, 13)$
32	$(11 \rightarrow 10 \rightarrow 3 \rightarrow 1 \rightarrow 2 \rightarrow 0)$	$(1, 0), (3, 0), (3, 2), (10, 0),$
		$(11, 0), (11, 1), (11, 2), (11, 3)$
33	$(11 \rightarrow 10 \rightarrow 3 \rightarrow 4 \rightarrow 6)$	$(3, 6), (11, 4), (11, 6)$
34	$(11 \rightarrow 8 \rightarrow 13 \rightarrow 10)$	$(11, 10)$
35	$(12 \rightarrow 13 \rightarrow 8 \rightarrow 7 \rightarrow 0)$	$(7, 0), (8, 0), (12, 0), (13, 0), (13, 7)$
36	$(12 \rightarrow 5 \rightarrow 2 \rightarrow 0 \rightarrow 1)$	$(12, 1)$
37	$(12 \rightarrow 11 \rightarrow 8 \rightarrow 7 \rightarrow 6 \rightarrow 4)$	$(7, 4), (8, 4), (11, 7), (11, 8),$
		$(12, 6), (12, 7)$
38	$(13 \rightarrow 10 \rightarrow 11 \rightarrow 8 \rightarrow 9)$	$(10, 8), (10, 9), (11, 9), (13, 9), (13, 11)$

TKN-10-002
Page 45

Bibliography

[Akim 99]   H. Akimaru and K. Kawashima. *Teletraffic: theory and applications*. Springer Verlag, 1999.

[As 94]   H. van As. "Media access techniques: The evolution towards terabit/s LANs and MANs". *Computer Networks and ISDN Systems*, Vol. 26, No. 6-8, pp. 603–656, 1994.

[Cple 03]   Cplex. "9.0 User's Manual". *ILOG, SA*, 2003.

[Epps 99]   D. Eppstein. "Finding the k shortest paths". *SIAM Journal on Computing*, Vol. 28, No. 2, pp. 652–673, 1999.

[Guma 04]   A. Gumaste and I. Chlamtac. "Light-trails: an optical solution for IP transport". *Journal of optical networking*, Vol. 3, No. 5, pp. 261–281, 2004. invited.

[Hu 05]   G. Hu, C. Gauger, and S. Junghans. "Performance of MAC layer and fairness protocol for the Dual Bus Optical Ring Network (DBORN)". *Proceedings of ONDM 2005*, pp. 467–476, 2005.

[Li 03]   J. Li and C. Qiao. "Schedule burst proactively for optical burst switched networks". In: *Proc. IEEE Globecom*, 2003.

[Mukh 06]   B. Mukherjee. *Optical WDM networks*. Springer-Verlag New York Inc, 2006.

[Pior 04]   M. Pióro and D. Medhi. *Routing, flow, and capacity design in communication and computer networks*. Morgan Kaufmann Publishers, 2004.

[Qiao 99]   C. Qiao and M. Yoo. "Optical burst switching (OBS)–a new paradigm for an optical internet". *Journal of high speed networks*, Vol. 8, No. 1, pp. 69–84, 1999.

[Rost 07]   A. Rostami and A. Wolisz. "Impact of edge traffic aggregation on the performance of FDL-assisted optical core switching nodes". In: *Proc. IEEE Int. Conf. Commun. (ICC)*, 2007.

[Rost 09]   A. Rostami, A. Wolisz, and A. Feldmann. "Traffic analysis in optical burst switching networks: a trace-based case study". *European Transactions on Telecommunications*, Vol. 20, No. 7, pp. 633–649, Nov. 2009. invited paper.

[Turn 99]   J. Turner. "Terabit burst switching". *Journal of High Speed Networks*, Vol. 8, No. 1, pp. 3–16, 1999.

[Varg 06]   A. Varga. "OMNeT++ Discrete event simulation system, User Manual". *Technical University of Budapest, Dept. of Telecommunications*, 2006.

[Widj 04]   I. Widjaja and I. Saniee. "Simplified layering and flexible bandwidth with TWIN". In: *Proceedings of the ACM SIGCOMM workshop on Future directions in network architecture*, pp. 13–20, 2004.

[Xion 00]   Y. Xiong, M. Vandenhoute, and H. C. Cankaya. "Control architecture in optical burst-switched WDM networks". *IEEE Journal on Selected Areas in Communications*, Vol. 18, pp. 1838–1851, 2000.